

Creation of Wave Packets for Quantum Chromodynamics on Quantum Computers

Matteo Turco,^{1, 2, 3, 4} Gonçalo Quinta,⁵ João Seixas,^{1, 2, 6, 4} and Yasser Omar^{1, 2, 7, 4}

¹*Physics of Information and Quantum Technologies Group,*

Centro de Física e Engenharia de Materiais Avançados (CeFEMA), Lisbon, Portugal

²*Laboratory of Physics for Materials and Emergent Technologies, Lisbon, Portugal*

³*Instituto Superior Técnico, Universidade de Lisboa, Lisbon, Portugal*

⁴*PQI – Portuguese Quantum Institute, Lisbon, Portugal*

⁵*Instituto de Telecomunicações, Lisbon, Portugal*

⁶*Departamento de Física, Instituto Superior Técnico, Universidade de Lisboa, Lisbon, Portugal*

⁷*Departamento de Matemática, Instituto Superior Técnico, Universidade de Lisboa, Lisbon, Portugal*

One of the most ambitious goals of quantum simulation of quantum field theory is the description of scattering in real time, which would allow not only for computation of scattering amplitudes, but also for studying the collision process step by step. The initial state of such simulation is made of typically two wave packets of stable particles moving on top of the vacuum, whose preparation is difficult. Here we extend a previous work to create wave packets of a general kind of particle from the vacuum in lattice gauge theories in various dimensions, including three-dimensional QCD for the first time. The conceptual foundation of this approach is the Haag-Ruelle scattering theory, and the only theoretical limitation is given by the presence of massless particles. In the context of digital quantum computation, the wave packet creation from the vacuum is implemented with the technique known as LCU (linear combination of unitaries). The preparation is performed successfully upon measuring an ancillary register with a certain probability, which vanishes polynomially in the lattice spacing, the wave-packet energy and the momentum narrowness.

I. INTRODUCTION

Quantum computation is a new promising paradigm to render feasible some computational problems that are classically too hard to be solved even with the huge amount of resources of the best supercomputers. More precisely, quantum computers are expected to have a truly strong impact in problems that require an exponentially large amount of classical resources and a polynomially large amount of quantum resources. For these problems, having a proper quantum computer would make the difference between solving relevant cases and not solving them. It would not be just a matter of making the computation faster. However, instances of such problems are rare. Of the few known examples, simulation of complex quantum systems, especially of strongly correlated many-body systems, is probably the most prominent. Traditional approaches, numerical or analytical, fail except in a handful of cases, or for limited classes of questions. For these reasons, quantum and quantum-inspired approaches are being widely studied [1–14].

A quantum field theory is essentially a strongly correlated quantum system with particular requirements on the symmetries it enjoys, namely Poincaré invariance. At a deep level, the correct implementation of this symmetry group also seems to demand gauge invariance to obtain nontrivial dynamics, at least in a three-dimensional space. A particularly challenging case is quantum chromodynamics (QCD), which describes the strong interaction between quarks and gluons. Differently from all the other sectors of the Standard Model of particle physics, a large part of its phenomenology is intrinsically nonperturbative, whence analytical techniques can be used only to set up the right framework for numerical calculations. The gauge group is $SU(3)$, which increases computational costs by several orders of magnitude with respect, for instance, to a $U(1)$ theory. Traditional lattice calculations are well suited to address problems in the imaginary-time formalism, such as prediction on particle masses and matrix elements, and information on the real-time evolution can be extracted in some cases [15]. However, general nonperturbative studies of processes in real-time evolution is one of the major open problems of particle physics.

For the reasons just mentioned, considerable effort within the quantum-computing and the high-energy-physics communities aims at simulating real-time evolution of processes within QCD [16–33]. The resources required to perform a useful quantum calculation in QCD are several orders of magnitude beyond the present capabilities [34], but promising progress has been made in the last years towards the realization of a large-scale, error-corrected quantum computer, both on the experimental and the theoretical side [35, 36]. Although a full quantum computer is still out of reach, it nonetheless makes sense to analyze all the possibilities to obtain realistic resource estimates, and determine which questions we will be able to address. Furthermore, on the long way to address full QCD there are many simpler theories, such as the Schwinger model, that can be used to test and benchmark new techniques, and to gain insight on some aspects of QCD and quantum field theory in general.

Specifically, we consider scattering of particles, a class of experiments which is extremely important for our understanding of fundamental physics. At very high energy, QCD is perturbative. The Lehmann-Symanzik-Zimmermann (LSZ) reduction formula [37] is a powerful tool to study cross sections at asymptotic times in perturbation theory and to obtain predictions to be tested against experimental results. However, at low energies, perturbation theory is no longer useful, so it is very challenging to study, for example, pion-pion or

proton-proton collisions above the inelastic-scattering threshold. The Haag-Ruelle formalism [38–40] is another excellent framework in which to study scattering. It was developed in the context of axiomatic quantum field theory, and it provides the logical link between the Wightman axioms and the LSZ reduction formula. While being a conceptual milestone of quantum field theory, it is not well suited for perturbative calculations, this being the main reason why it was outshone by the LSZ formalism. However, quantum computation may be the missing element to exploit the Haag-Ruelle theory in a practical way too, as we will shortly see.

Quantum simulation offers a possibility to study the real-time evolution of scattering processes, but compared to other applications, the initial state preparation is particularly difficult. In the framework of the Hamiltonian formulation on a spatial lattice, our goal is to prepare two wave packets of stable particles on top of the vacuum. If the goal is just to compute scattering amplitudes, wave packet preparation can be avoided [41, 42]. However, simulation of wave-packet collisions would allow for much more than computation of scattering amplitudes. We could directly monitor the dynamics step by step, and gain insight on what happens during the collision, which is not easily accessible even in perturbative regimes.

Concerning the preparation of wave packets, the key step in the first proposed approaches consists of a modified adiabatic transformation to turn wave packets of the free theory into wave packets of the interacting theory [43–47]. Since in the free theory there are no states corresponding to composite particles, this method can only be used for particles associated with elementary degrees of freedom. As a consequence of confinement in QCD, no quarks or gluons appear in the spectrum, and all the particles (hadrons) are composite. Therefore, the approach used in [43–47] does not apply to QCD.

To circumvent the problem, other strategies have to be followed. Several ideas have been discussed and explored numerically in one dimension. In [48, 49], variational algorithms are used to obtain wave packets in a scalar-field theory. Variational approaches are also used in the Schwinger model in [50]. Preparation of W states combined with variational techniques is used in [51], which works well in models with a short correlation length and, thus, far from the continuum limit. In the context of the Abelian gauge theories Z_2 and $U(1)$, ideas based on ansatz-optimization [52, 53] or quantum subspace expansion [54] have been proposed to obtain operators that create mesonic wave packets from the interacting vacuum, similarly to what is done in [2] using tensor networks and in [55] for the Thirring model. Generalization of these methods to more complicated cases, such as mesonic and baryonic particles in multidimensional non-Abelian theories, is possible in principle, but it has to be shown that these methods remain efficient when more complicated structures are considered, and when larger wave packets in coordinate space are needed to obtain more energetic wave packets with a narrower distribution in momentum space in the continuum limit. In [50], another idea is proposed for theories displaying confinement: wave packets are adiabatically transformed from the strong-coupling limit to the full theory, rather than from the free theory. This should avoid the issue explained in the previous paragraph, but more investigation is required. A possible problem is that in the continuum limit a theory like QCD is weakly coupled due to asymptotic freedom, and the adiabatic transformation may be difficult to implement.

A general approach, based on the Haag-Ruelle scattering theory, has been introduced in our previous work [56], where we described how to obtain creation operators for elementary and composite particles in interacting scalar-field theories. These operators act on the interacting vacuum, so efficient interacting-vacuum preparation is assumed to be available. Another required ingredient is knowledge of the spectrum. The only theoretical limitation of this strategy is the existence of an isolated mass shell, which should be guaranteed by a finite mass gap in the continuum limit. Apart from this, it is easily adaptable to different theories, different formulations, and different particles, as we show in this work. The creation operators are obtained by appropriately smearing interpolating operators for a given particle over space and time. Its asymptotic efficiency can be shown in the continuum limit and for high-energy wave packets with narrow distribution in momentum space. The main difficulty is that it only succeeds upon measuring an ancillary register of qubits with a certain outcome. The success probability is polynomially vanishing in the lattice spacing, the wave-packet energy and the momentum narrowness.

In the present work, we show how to apply the method based on the Haag-Ruelle formalism [56] to QCD. We provide the first description of an efficient strategy to prepare wave packets in this theory, assuming there is an efficient way to prepare the vacuum state. Apart from addressing theories different from our previous work [56], the new aspects we address here concern how to deal with particles with spin one-half and higher, how to write interpolating operators in terms of qubit operators, and estimating the success probability for different particles. To achieve this, we bring together tools and concepts from different areas of research developed over several decades, ranging from axiomatic quantum field theory, traditional lattice field theory and Hamiltonian formulation of lattice theories to quantum computation. As a warm up, we consider $U(1)$, $SU(2)$ and $SU(3)$ theories in one dimension. We use them to introduce some building blocks required for three-dimensional QCD. Moreover, the simulation of these theories requires much less resources than full QCD, and they are often used as toy models to test ideas. Treating them separately from QCD may be useful for implementations in the near or mid-term future. We focus, for simplicity, on the well-known pions and nucleons. Other kinds of particles can be treated in a completely analogous way.

It is not clear which formulation of lattice QCD will be best suited for quantum simulation, but a common choice has been the Kogut-Susskind formulation, a choice we henceforth follow. Other possibilities are the loop-string-hadron formulation [57–60], or the Wilson-fermion formulation [61]. The former is based on the

Kogut-Susskind formulation, so developing tools for the Kogut-Susskind formulation is typically necessary or useful also for the loop-string-hadron one. Porting the tools developed in this paper to the Wilson-fermion formulation is straightforward. Another option is to use the orbifold formulation [62, 63], which can also be connected to the Kogut-Susskind framework. Therefore, the choice of the Kogut-Susskind formulation is actually quite general.

The rest of this paper is organized as follows. In section II, we review the approach presented in [56], and we extend it to particles of general spin. In section III we give the lattice operators that are necessary for the creation of wave packets in one-dimensional lattice gauge theories $U(1)$, $SU(2)$ and $SU(3)$. In section IV we show how to implement the same operators in terms of qubit operators. Finally, in section V we consider two-flavoured QCD in three dimensions, and in section VI we give our conclusions. In the appendix we review the generalized superfast encoding of fermions onto qubits, and we also show how to implement odd operators.

II. CREATION OF WAVE PACKETS FROM THE VACUUM

In this section we briefly review the main features of the method proposed in [56], based on the Haag-Ruelle scattering theory, to create wave packets of particles in an interacting field theory from the vacuum of the theory. In [56] scalar-field theories were considered, while in this paper we take at first a more general view. Then, at the end of the section, we focus on spin-one-half particles, and give some results that are necessary to determine the complexity of the method. The Haag-Ruelle formulation [38, 39] was originally developed in axiomatic quantum field theory and recently formalized for lattice systems [64]. For a thorough review of the formulation in the continuum see [40], whose extensive explanation goes perhaps beyond the purposes of quantum simulation. We invite the reader interested in quantum simulation to go through [56], which also includes a more concise review of the Haag-Ruelle formalism.

For our purposes, the relevant result is that we can create wave packets of a certain particle using operators of the form

$$\hat{a}_\psi^\dagger = \int d^D x \psi(x) \hat{\mathcal{O}}(x), \quad (1)$$

where $D = d + 1$ is the number of spacetime dimensions, x is a spacetime coordinate, ψ is a Schwartz function, and $\hat{\mathcal{O}}$ is an interpolating Heisenberg operator for the particle we want to create. The function ψ and the operator $\hat{\mathcal{O}}$ have to be properly chosen considering the spectrum and the symmetries of the theory. The operator in equation (1) is sometime called a Haag-Ruelle creation operator. For proper choices of ψ and $\hat{\mathcal{O}}$, the state $\hat{a}_\psi^\dagger |\Omega\rangle$, where $|\Omega\rangle$ denotes the vacuum, is a one-particle state. To create multiple wave packets in different space regions, we just need to apply multiple Haag-Ruelle creation operators with spatially separated functions ψ_1, ψ_2, \dots . Intuitively, the function ψ is responsible for selecting one-particle states and cutting off multiparticle states. The operator $\hat{\mathcal{O}}$ is responsible for selecting the desired kind of particle. Some examples should help to understand these points.

To begin, suppose we have a theory with only one particle of mass m in the spectrum. The momentum operators $P_0 = H$ and $P_i, i = 1, \dots, d$, commute with each other, so we can consider their joint spectrum. This is made of three separate sectors:

- the vacuum, corresponding to the origin, $p_\mu = 0$;
- the one-particle mass hyperboloid, given by the points such that $p_\mu p^\mu = m^2$;
- the multiparticle continuum, defined by $p_\mu p^\mu \geq 4m^2$.

The function ψ is chosen as the Fourier transform of a function $\tilde{\psi}$ with support overlapping only with the one-particle mass hyperboloid, and not with the multiparticle continuum, as depicted in figure 1a.

The interpolating operator $\hat{\mathcal{O}}$ should carry the same quantum numbers as the particle. More precisely, if $|\alpha\rangle$ is a one-particle state and $|\Omega\rangle$ the vacuum, then the condition for $\hat{\mathcal{O}}$ to be an interpolating operator is

$$\langle \alpha | \hat{\mathcal{O}} | \Omega \rangle \neq 0. \quad (2)$$

As a second example, suppose there are two particles of masses m_1 and m_2 . Our goal is to create wave packets of a definite kind of particle, and not a mixture of the two. If m_2 lies halfway between m_1 and $2m_1$, this can be achieved by choosing $\tilde{\psi}$ with support only on the mass hyperboloid of one kind of particle, namely either around $p_\mu p^\mu = m_1^2$ or $p_\mu p^\mu = m_2^2$. If m_2 is close to m_1 , close to $2m_1$, or is larger than $2m_1$, then the operator $\hat{\mathcal{O}}$ must be chosen to be an interpolating operator only for one kind of particle, and not for the other. For example, we could have

$$\langle \alpha_1 | \hat{\mathcal{O}} | \Omega \rangle \neq 0, \quad \langle \alpha_2 | \hat{\mathcal{O}} | \Omega \rangle = 0, \quad (3)$$

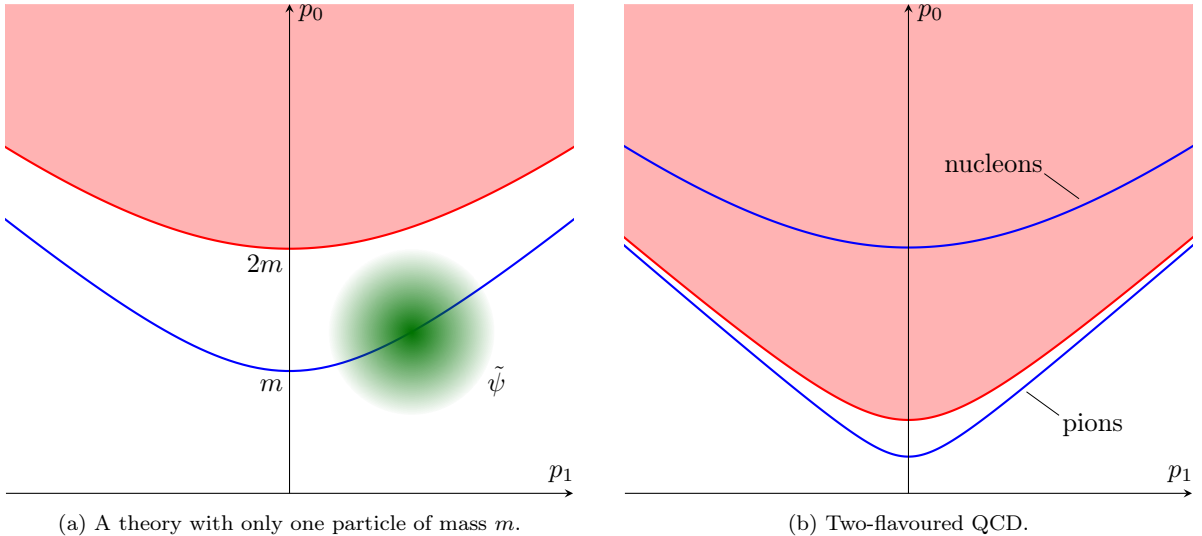


FIG. 1: Two examples of the joint energy-momentum spectrum in continuum quantum field theory. The blue lines represent the one-particle mass hyperboloids, the red regions are the multiparticle continua, and the green spot represents the support of the function ψ . For visual clarity, only one spatial component is shown.

where $|\alpha_i\rangle$ is a state of particle i . The way to identify particles, and hence appropriate interpolating operators, is through symmetry considerations: the interpolating operator should carry the same quantum numbers as the particle in consideration.

Finally, we can consider QCD with two flavours of quarks. The low-lying spectrum is depicted in figure 1b, where only one spatial component is shown for visual clarity. The fact that the one-nucleon mass hyperboloid lies in the multipion continuum is not a problem because the two kind of particles have different spins and isospins.

On a lattice, the same ideas apply with due modifications. Coordinate space and momentum space are discretized, while time is left continuous. Spectra are distorted, but should still contain separate one-particle and multiparticle sectors. We may then rewrite equation (1) on a lattice with spacing a as

$$\hat{a}_\psi^\dagger = \sum_{\mathbf{x}} a^d \int_{-\infty}^{+\infty} dt \psi(t, \mathbf{x}) e^{iHt} \hat{\mathcal{O}}(\mathbf{x}) e^{-iHt}, \quad (4)$$

where $\hat{\mathcal{O}}(\mathbf{x})$ is the Schrödinger representation of $\hat{\mathcal{O}}(x)$, and $x = (t, \mathbf{x})$. When moving from the continuum to the lattice, many symmetries are lost, and new particles may appear. As a consequence, there arises the problem of identifying particles and using the correct lattice interpolators. We deal with this more in detail in section V.

The lattice theory has to be mapped onto a qubit system, with all due truncation and digitization [65, 66]. Also the time integral in equation (4) has to be approximated by a discrete and truncated summation in steps of δ_t over N points,

$$\hat{a}_\psi^\dagger = \sum_{\mathbf{x}} \sum_{i=1}^N a^d \delta_t \psi(t_i, \mathbf{x}) e^{iHt_i} \hat{\mathcal{O}}(\mathbf{x}) e^{-iHt_i}. \quad (5)$$

The required number of time samples can be shown to grow like

$$N = O\left(\frac{T}{\sqrt{\epsilon}} \sqrt{\|[H, [H, \hat{\mathcal{O}}(\mathbf{x})]]\|}\right), \quad (6)$$

where T is the size of ψ in the time direction, and ϵ is the error introduced by the time-integral discretization. On a quantum computer, we can only implement operators with $\|\hat{\mathcal{O}}\| = O(1)$. Assuming the Hamiltonian is a sum of local terms, $H = \sum_{\mathbf{x}} H(\mathbf{x})$, we conclude that

$$N = O\left(\frac{T}{\sqrt{\epsilon}} \|H(\mathbf{x})\|\right). \quad (7)$$

Notice that N does not depend on the lattice size.

Once we know how to implement $\hat{\mathcal{O}}$ on a quantum computer, the creation operator \hat{a}_ψ^\dagger can be implemented by means of a linear combination of unitaries (LCU) [67]. If S is the number of lattice sites in the support of ψ , this

requires an ancillary register of $\log_2(NS)$ qubits, NS calls to controlled versions of $\hat{\mathcal{O}}$, and time evolution for a time $O(T)$. The time evolution is likely the most expensive part in the implementation of \hat{a}_ψ^\dagger , since N depends only on the local terms of the Hamiltonian, while the time evolution depends on the whole Hamiltonian. Also, the local operators $\hat{\mathcal{O}}$ we consider in this work are not hard to implement.

The interpolator $\hat{\mathcal{O}}(\mathbf{x})$ is typically not unitary, so it has to be block encoded. Since any operator on a qubit system can be expanded as a linear combination of unitary operators, in general we can use LCU,

$$\hat{\mathcal{O}}(\mathbf{x}) = \sum_{j=1}^L c_j \mathcal{U}_j(\mathbf{x}), \quad \sum_j |c_j| = C, \quad c_j \in \mathbb{C}. \quad (8)$$

In the cases we consider below, L is a constant depending only on the kind of particle and the theory. Another $\log_2 L$ ancillary qubits are required to implement $\hat{\mathcal{O}}(\mathbf{x})$. The quantity C depends on L and on the mass dimension of the interpolator.

Overall, \hat{a}_ψ^\dagger is successfully implemented upon measurement of the ancillary register with probability

$$\rho = \left(\frac{\|\hat{a}_\psi^\dagger|\Omega\rangle\|}{\alpha} \right)^2, \quad \text{where } \alpha = C \sum_{\mathbf{x}, t} a^d \delta_t |\psi(t, \mathbf{x})|. \quad (9)$$

The success probability determines the efficiency of our method for wave-packet preparation. If we want to create two wave packets, with success probabilities ρ_1 and ρ_2 , we need to repeat the vacuum preparation and wave-packet creation about $1/(\rho_1 \rho_2)$ times before succeeding. This can be quadratically improved applying amplitude amplification [68].

If the operator $\hat{\mathcal{O}}(x)$ is a scalar field, the analysis in [56] shows that the behavior of ρ is

$$\rho \sim \frac{Z}{C^2} \frac{\delta_p^d}{\bar{E}}, \quad (10)$$

where δ_p is the linear size of the support of $\tilde{\psi}$ in the spatial components of the momentum, \bar{E} is the energy of the particle, and Z is the squared renormalization constant connecting $\hat{\mathcal{O}}(\mathbf{x})$ with its continuum normalization, typically logarithmic in the lattice spacing [69].

In general, $\hat{\mathcal{O}}(x)$ can be a spinorial field (or another kind of field), as is the case for the proton, and the result has to be adapted. Assume that under a Lorentz transformation in the continuum we have $\hat{\mathcal{O}}_\alpha \rightarrow \sum_\beta S(\Lambda)_{\alpha\beta} \hat{\mathcal{O}}_\beta$, and that the operators $\hat{\mathcal{O}}_\alpha$ interpolate for a particle of spin J and mass m . There are $2J+1$ one-particle states with momentum \mathbf{k} , $|\mathbf{k}, j\rangle$, with $j = -J, -J+1, \dots, J$. Then we have

$$\|\hat{a}_{\alpha, \psi}^\dagger|\Omega\rangle\|^2 = \int d^3k |\tilde{\psi}(\mathbf{k})|^2 \frac{m}{E(\mathbf{k})} \sum_j \left| \sum_\beta S(\Lambda_{\mathbf{k}})_{\alpha\beta} \sqrt{Z_\beta^j} \right|^2, \quad (11)$$

where $E(\mathbf{k}) = \sqrt{|\mathbf{k}|^2 + m^2}$, $\tilde{\psi}(\mathbf{k}) = \tilde{\psi}(E(\mathbf{k}), \mathbf{k})$, $\sqrt{Z_\beta^j} = \langle \mathbf{0}, j | \hat{\mathcal{O}}_\beta(0) | \Omega \rangle$, and $\Lambda_{\mathbf{k}}$ is the boost that sends \mathbf{k} to $\mathbf{0}$. If $\tilde{\psi}$ is narrowly concentrated around $\bar{\mathbf{k}}$, then we roughly have $S(\Lambda_{\mathbf{k}}) \sim S(\Lambda_{\bar{\mathbf{k}}})$ in equation (11). Therefore, in equation (10), we can replace Z with

$$Z \rightarrow \sum_j \left| \sum_\beta S(\Lambda_{\bar{\mathbf{k}}})_{\alpha\beta} \sqrt{Z_\beta^j} \right|^2. \quad (12)$$

We consider now the example of a spinorial field in the Dirac representation interpolating for a spin-one-half particle with momentum $\bar{\mathbf{k}} = (k_x, 0, 0)$. We have

$$S(\Lambda_{\bar{\mathbf{k}}}) = \begin{pmatrix} \sqrt{\frac{\gamma+1}{2}} \mathbb{1} & \sqrt{\frac{\gamma-1}{2}} \sigma_x \\ \sqrt{\frac{\gamma-1}{2}} \sigma_x & \sqrt{\frac{\gamma+1}{2}} \mathbb{1} \end{pmatrix}, \quad \gamma = \frac{E(\bar{\mathbf{k}})}{m}. \quad (13)$$

Then, for $k_x \gg m$, we have

$$\sum_\beta S(\Lambda_{\bar{\mathbf{k}}})_{\alpha\beta} \sqrt{Z_\beta^j} = \frac{1}{\sqrt{2}} \sqrt{\frac{k_x}{m}} \left(\sqrt{Z_1^j} - \sqrt{Z_4^j} \right) + \frac{1}{2\sqrt{2}} \sqrt{\frac{m}{k_x}} \left(\sqrt{Z_1^j} + \sqrt{Z_4^j} \right) + \dots \quad (14)$$

Notice that, for a spinorial interpolator, and if $Z_1^j \neq Z_4^j$, the term k_x/m from this expansion compensates the term \bar{E} in the numerator of equation (10) for highly energetic spin-one-half particles. If instead $Z_1^j = Z_4^j$, then we need to consider the second term in the expansion, which brings another suppression factor of $1/\bar{E}$ in the success probability.

In this section we have discussed the general features of how to prepare wave packets on quantum computers using the Haag-Ruelle scattering theory, focusing on particles of spin zero and one half. To continue the discussion, we need to consider specific examples. In particular, we need to have explicit expressions for the interpolating operators to estimate the quantity C in (9). This is the content of the following sections.

III. INTERPOLATING OPERATORS IN ONE-DIMENSIONAL LATTICE GAUGE THEORIES

In this and the following sections, we aim at showing how to decompose interpolating operators into a linear combination of unitaries on qubit systems, providing some rough estimates on the resources needed and the success probability. We start by considering the simpler case of gauge theories in one space dimension, which is enough to show all the building blocks that are necessary in the physical case of quantum chromodynamics.

The Kogut-Susskind Hamiltonians for lattice gauge theories $U(1)$, $SU(2)$ and $SU(3)$ in one space dimension can be compactly written as [70]

$$H = \sum_{x=0}^{N-1} \left[\frac{i}{2a} (\xi^\dagger(x+1)U(x)\xi(x) - \xi^\dagger(x)U^\dagger(x)\xi(x+1)) + (-1)^x m_0 \xi^\dagger(x)\xi(x) + \frac{ag_0^2}{2} E(x)^2 \right]. \quad (15)$$

When referring to the $U(1)$ theory, $\xi(x)$, $U(x)$ and $E(x)$ are one-component fields. When referring to the $SU(2)$ theory, the same symbols mean

$$\xi(x) = \begin{pmatrix} \xi_1(x) \\ \xi_2(x) \end{pmatrix}, \quad U(x) = \begin{pmatrix} U_{11}(x) & U_{12}(x) \\ U_{21}(x) & U_{22}(x) \end{pmatrix}, \quad E(x)^2 = \sum_{a=1}^3 E_L^a(x)^2 = \sum_{a=1}^3 E_R^a(x)^2. \quad (16)$$

When referring to the $SU(3)$ theory, the symbols mean

$$\xi(x) = \begin{pmatrix} \xi_1(x) \\ \xi_2(x) \\ \xi_3(x) \end{pmatrix}, \quad U(x) = \begin{pmatrix} U_{11}(x) & U_{12}(x) & U_{13}(x) \\ U_{21}(x) & U_{22}(x) & U_{23}(x) \\ U_{31}(x) & U_{32}(x) & U_{33}(x) \end{pmatrix}, \quad E(x)^2 = \sum_{a=1}^8 E_L^a(x)^2 = \sum_{a=1}^8 E_R^a(x)^2. \quad (17)$$

In these formulations we use staggered fermions. A relevant caveat is that only even lattice translations can be interpreted as space translations in the continuum. Translations that involve an odd number of lattice units in one or more directions do not correspond to space translations in the continuum, but to other transformations that are not necessarily symmetries of the theory. Hence, the summation over \mathbf{x} in equation (4) should be in steps of two, as in

$$\hat{a}_\psi^\dagger = \sum_{x=0}^{\frac{N}{2}-1} 2a \int_{-\infty}^{+\infty} dt \psi(t, 2x) e^{iHt} \hat{O}(2x) e^{-iHt}. \quad (18)$$

A. $U(1)$ gauge theory

For the $U(1)$ gauge theory, also known as the Schwinger model, the fields satisfy the following anticommutation and commutation relations:

$$\{\xi(x), \xi^\dagger(y)\} = \delta_{xy}, \quad [U(x), E(y)] = \delta_{xy} U(x). \quad (19)$$

The local Hilbert space of the gauge field can be expressed in the electric-field basis $\{|\mathcal{E}\rangle : \mathcal{E} \in \mathbb{Z}\}$, in which we have

$$E|\mathcal{E}\rangle = \mathcal{E}|\mathcal{E}\rangle, \quad U|\mathcal{E}\rangle = |\mathcal{E}-1\rangle. \quad (20)$$

In this model there are three stable mesons in the continuum limit, with associated interpolating operators [71]

$$\bar{\psi}\psi, \quad \psi^\dagger\gamma_5\psi, \quad i\bar{\psi}\gamma_5\psi. \quad (21)$$

The Dirac spinor ψ for the quark field has two components in one dimension. In the staggered-fermion formulation, the upper component is identified with fermionic modes at even sites, while the lower component is identified with fermionic modes at odd sites. Furthermore, the dimensionless field ξ has to be multiplied by a factor $1/\sqrt{a}$ to match the continuum normalization, $\psi \sim \xi/\sqrt{a}$. The operators in equation (21) translate respectively to

$$\hat{O}_1(x) = \frac{1}{a} [\xi^\dagger(x)\xi(x) - \xi^\dagger(x+1)\xi(x+1)], \quad (22)$$

$$\hat{O}_2(x) = \frac{1}{a} [\xi^\dagger(x)U^\dagger(x)\xi(x+1) + \xi^\dagger(x+1)U(x)\xi(x)], \quad (23)$$

$$\hat{O}_3(x) = \frac{1}{a} [\xi^\dagger(x)U^\dagger(x)\xi(x+1) - \xi^\dagger(x+1)U(x)\xi(x)], \quad (24)$$

where we have dropped the factor i in \hat{O}_3 as it is irrelevant for our purposes.

B. $SU(2)$ gauge theory

The anticommutation and commutation relations for the $SU(2)$ gauge theory are

$$\{\xi_\alpha(x), \xi_\beta^\dagger(y)\} = \delta_{xy}\delta_{\alpha\beta}, \quad [U_{\alpha\beta}(x), E_L^a(y)] = \delta_{xy}T_{\alpha\gamma}^a U_{\gamma\beta}(x), \quad [U_{\alpha\beta}(x), E_R^a(y)] = -\delta_{xy}U_{\alpha\gamma}(x)T_{\gamma\beta}^a, \quad (25)$$

where $T^a = \sigma^a/2$. We adopt the Einstein summation convention for repeated indices. Latin indices like a, b, c, \dots run over $\{1, 2, 3\}$ for $SU(2)$ and over $\{1, 2, \dots, 8\}$ for $SU(3)$, while Greek indices like $\alpha, \beta, \gamma, \dots$ run over $\{1, 2\}$ for $SU(2)$ and over $\{1, 2, 3\}$ for $SU(3)$. In addition we have $U_{11}^\dagger(x) = U_{22}(x)$ and $U_{21}^\dagger(x) = -U_{12}(x)$.

A basis for the local Hilbert space of the gauge field is given by

$$|j, m_L, m_R\rangle, \quad j = 0, \frac{1}{2}, 1, \dots, \quad m_L, m_R = -j, -j+1, \dots, j, \quad (26)$$

in which the operators E^2 , E_L^3 and E_R^3 are diagonal and give

$$E^2|j, m_L, m_R\rangle = j(j+1)|j, m_L, m_R\rangle, \quad (27)$$

$$E_L^3|j, m_L, m_R\rangle = m_L|j, m_L, m_R\rangle, \quad E_R^3|j, m_L, m_R\rangle = m_R|j, m_L, m_R\rangle. \quad (28)$$

The operators $U_{\alpha\beta}$ can be expressed as

$$U_{\alpha\beta}|j, m_L, m_R\rangle = c_{\alpha\beta}^-(j, m_L, m_R)|j - \frac{1}{2}, m_L + \frac{3}{2} - \alpha, m_R + \frac{3}{2} - \beta\rangle + c_{\alpha\beta}^+(j, m_L, m_R)|j + \frac{1}{2}, m_L + \frac{3}{2} - \alpha, m_R + \frac{3}{2} - \beta\rangle, \quad (29)$$

where $c_{\alpha\beta}^\pm(j, m_L, m_R)$ are products of Clebsch-Gordan coefficients,

$$c_{\alpha\beta}^\pm(j, m_L, m_R) = \sqrt{\frac{2j+1}{2j+1+1}}\langle j \pm \frac{1}{2}, m_L + \frac{3}{2} - \alpha | j, m_L; \frac{1}{2}, \frac{3}{2} - \alpha \rangle \langle j \pm \frac{1}{2}, m_R + \frac{3}{2} - \beta | j, m_R; \frac{1}{2}, \frac{3}{2} - \beta \rangle. \quad (30)$$

We also have the decomposition

$$U_{\alpha\beta} = M_\alpha^L M_\beta^R (J^- c_{\alpha\beta}^- + J^+ c_{\alpha\beta}^+), \quad (\text{no summation over } \alpha \text{ and } \beta) \quad (31)$$

with

$$M_\alpha^L|j, m_L, m_R\rangle = |j, m_L + \frac{3}{2} - \alpha, m_R\rangle, \quad (32)$$

$$M_\beta^R|j, m_L, m_R\rangle = |j, m_L, m_R + \frac{3}{2} - \beta\rangle, \quad (33)$$

$$J^\pm|j, m_L, m_R\rangle = |j \pm \frac{1}{2}, m_L, m_R\rangle, \quad (34)$$

$$c_{\alpha\beta}^\pm|j, m_L, m_R\rangle = c_{\alpha\beta}^\pm(j, m_L, m_R)|j, m_L, m_R\rangle. \quad (35)$$

Analogously to the $U(1)$ theory, the $SU(2)$ theory has mesons [72]

$$\hat{\mathcal{O}}_1(x) = \frac{1}{a} [\xi^\dagger(x)\xi(x) - \xi^\dagger(x+1)\xi(x+1)], \quad (36)$$

$$\hat{\mathcal{O}}_2(x) = \frac{1}{a} [\xi^\dagger(x)U^\dagger(x)\xi(x+1) + \xi^\dagger(x+1)U(x)\xi(x)], \quad (37)$$

$$\hat{\mathcal{O}}_3(x) = \frac{1}{a} [\xi^\dagger(x)U^\dagger(x)\xi(x+1) - \xi^\dagger(x+1)U(x)\xi(x)]. \quad (38)$$

In addition, it has a baryon,

$$\hat{\mathcal{O}}_4(x) = \frac{1}{a} \epsilon_{\alpha\beta} \xi_\alpha^\dagger(x) \xi_\beta^\dagger(x), \quad (39)$$

where $\epsilon_{\alpha\beta}$ is the Levi-Civita symbol. However, the baryon is expected to coincide with a meson in the continuum limit.

C. $SU(3)$ gauge theory

The $SU(3)$ case is a more complicated version of the $SU(2)$ one. For the details see [70]. The basis states are labeled by eight quantum numbers

$$|p, q, T_L, T_L^z, Y_L, T_R, T_R^z, Y_R\rangle, \quad (40)$$

$$p, q = 0, 1, 2, \dots, \quad T_{L/R} = 0, \frac{1}{2}, \dots, \frac{1}{2}(p+q), \quad (41)$$

$$T_{L/R}^z = -\frac{1}{2}(p+q), -\frac{1}{2}(p+q+1), \dots, \frac{1}{2}(p+q), \quad Y_{L/R} = -\frac{1}{3}(q+2p), -\frac{1}{3}(q+2p+1), \dots, \frac{1}{3}(p+2q). \quad (42)$$

Similarly to the $SU(2)$ case, in this basis we have the decomposition

$$U_{\alpha\beta} = M_\alpha^L M_\beta^R (P^+ \mathcal{C}_{1\alpha}^L \mathcal{C}_{1\beta}^R \hat{N}_1 + P^- Q^+ \mathcal{C}_{2\alpha}^L \mathcal{C}_{2\beta}^R \hat{N}_2 + Q^- \mathcal{C}_{3\alpha}^L \mathcal{C}_{3\beta}^R \hat{N}_3), \quad (\text{no summation over } \alpha \text{ and } \beta) \quad (43)$$

where ($i = L, R$)

$$M_1^i |T_i^z, Y_i\rangle = |T_i^z + \frac{1}{2}, Y_i + \frac{1}{3}\rangle, \quad M_2^i |T_i^z, Y_i\rangle = |T_i^z - \frac{1}{2}, Y_i + \frac{1}{3}\rangle, \quad M_3^i |T_i^z, Y_i\rangle = |T_i^z, Y_i - \frac{2}{3}\rangle, \quad (44)$$

$$P^\pm |p, q\rangle = |p \pm 1, q\rangle, \quad Q^\pm |p, q\rangle = |p, q \pm 1\rangle, \quad T_i^\pm |T_i\rangle = |T_i \pm \frac{1}{2}\rangle, \quad (45)$$

$$\mathcal{C}_{\alpha 1}^i = T_i^+ \hat{C}_{\alpha 1}^{i(a)} + T_i^- \hat{C}_{\alpha 1}^{i(b)}, \quad \mathcal{C}_{\alpha 2}^i = T_i^+ \hat{C}_{\alpha 2}^{i(a)} + T_i^- \hat{C}_{\alpha 2}^{i(b)}, \quad \mathcal{C}_{\alpha 3}^i = \hat{C}_{\alpha 3}^i, \quad (46)$$

and the diagonal operators $\hat{N}_{1,2,3}$, $\hat{C}_{\alpha\beta}^{i(a,b)}$ and $\hat{C}_{\alpha 3}^i$ can be found in [70].

As for the $SU(2)$ case, we can suppose that the $SU(3)$ theory has mesons of the form of Φ_i in equations (36)-(38), but baryons are actually fermionic particles in this case,

$$\hat{\mathcal{O}}_4(x) = \frac{1}{a^{3/2}} \epsilon_{\alpha\beta\gamma} \xi_\alpha^\dagger(x) \xi_\beta(x) \xi_\gamma^\dagger(x). \quad (47)$$

IV. INTERPOLATING OPERATORS ON QUBITS

The theories and the operators discussed in the previous section need to be mapped to a qubit system. In one dimension, the Jordan-Wigner transformation works well to map fermionic operators to qubit operators. More specifically we choose the following orderings:

$$\xi(x) \rightarrow \sigma^z(0) \cdots \sigma^z(x-1) \sigma^+(x) \quad \text{for } U(1), \quad (48)$$

$$\left. \begin{aligned} \xi_1(x) &\rightarrow \sigma_1^z(0) \sigma_2^z(0) \sigma_1^z(1) \cdots \sigma_2^z(x-1) \sigma_1^+(x) \\ \xi_2(x) &\rightarrow \sigma_1^z(0) \sigma_2^z(0) \sigma_1^z(1) \cdots \sigma_2^z(x-1) \sigma_1^z(x) \sigma_2^+(x) \end{aligned} \right\} \quad \text{for } SU(2), \quad (49)$$

$$\left. \begin{aligned} \xi_1(x) &\rightarrow \sigma_1^z(0) \sigma_2^z(0) \sigma_3^z(0) \sigma_1^z(1) \cdots \sigma_3^z(x-1) \sigma_1^+(x) \\ \xi_2(x) &\rightarrow \sigma_1^z(0) \sigma_2^z(0) \sigma_3^z(0) \sigma_1^z(1) \cdots \sigma_3^z(x-1) \sigma_1^z(x) \sigma_2^+(x) \\ \xi_3(x) &\rightarrow \sigma_1^z(0) \sigma_2^z(0) \sigma_3^z(0) \sigma_1^z(1) \cdots \sigma_3^z(x-1) \sigma_1^z(x) \sigma_2^z(x) \sigma_3^+(x) \end{aligned} \right\} \quad \text{for } SU(3), \quad (50)$$

where $\sigma^\pm = (\sigma^x \pm i\sigma^y)/2$.

On the other hand, the local Hilbert space of the gauge field needs to be truncated. For $U(1)$ this is quite simple: if we use k qubits for a single link, then we impose the cutoff $\Lambda = 2^{k-1}$ and we encode the states $|\Lambda\rangle, |\Lambda+1\rangle, \dots, |\Lambda-1\rangle$ in the computational basis. The operator U needs to be adapted to the truncation. A common choice is to take

$$\begin{aligned} U|\mathcal{E}\rangle &= |\mathcal{E}-1\rangle, \quad \text{for } \mathcal{E} = -\Lambda+1, \dots, \Lambda-1, \\ U|\Lambda\rangle &= |\Lambda-1\rangle. \end{aligned} \quad (51)$$

In this way U is a permutation operator and can be implemented on a qubit system using $O(k^3)$ gates and no ancillary qubit, or using $O(k^2)$ gates and $k-1$ ancillary qubits. For $SU(2)$ and $SU(3)$ the situation is more complicated but similar in essence. We refer the reader to [70] for the details. After imposing a cutoff Λ , the permutation operators $M_\alpha^{L/R}$, J^\pm of $SU(2)$, and $M_\alpha^{L/R}$, P^\pm , Q^\pm , $T_{L/R}^\pm$ of $SU(3)$, take the same form as U in equation (51).

The diagonal operators $c_{\alpha\beta}^\pm$ in (31) and the ones in (43), like for instance $\hat{C}_{11}^{\text{L}(a)}\hat{C}_{11}^{\text{R}(a)}\hat{N}_1$, are not unitary. However, their entries lie between -1 and 1 , and are efficiently computable classically. We can implement them in the following way: suppose that the function $f(x)$, where x can take M values encoded in the computational basis, is efficiently computable with classical techniques, and take an ancillary register of $\eta = O(\log_2 M)$ qubits initialized in the state

$$|F\rangle = \frac{1}{\sqrt{N}} \sum_{n=0}^{N-1} e^{-i2\pi n/N} |n\rangle, \quad N = 2^\eta. \quad (52)$$

Then we can build efficient quantum circuits to implement unitary operators U_f^\pm such that

$$U_f^\pm |x\rangle |F\rangle = e^{\pm if(x)} |x\rangle |F\rangle. \quad (53)$$

We can use LCU to combine the two operators and obtain

$$\frac{(U_f^+ - U_f^-)}{2i} |x\rangle |F\rangle = \sin[f(x)] |x\rangle |F\rangle. \quad (54)$$

Going back to our case, denote by \mathcal{D} a diagonal operator, and by $\mathcal{D}(x)$ its entries, with $x = (j, m_L, m_R)$ for $SU(2)$, and $x = (p, q, T_L, T_L^z, Y_L, T_R, T_R^z, Y_R)$ for $SU(3)$. Then, taking $f(x) = \arcsin[\mathcal{D}(x)]$, we can implement \mathcal{D} . In this way we can write $U_{\alpha\beta}$ as a linear combination of unitary operators, and we can use LCU to implement it.

We can now write the interpolating operators in the qubit system, together with the corresponding quantity C defined in equation (8). For $U(1)$ they take the form

$$\hat{\mathcal{O}}_1(x) = \frac{1}{a} [\sigma^+(x)\sigma^-(x) - \sigma^+(x+1)\sigma^-(x+1)], \quad C_1 = \frac{2}{a}, \quad (55)$$

$$\hat{\mathcal{O}}_2(x) = \frac{1}{a} [\sigma^-(x)U^\dagger(x)\sigma^+(x+1) + \sigma^-(x+1)U(x)\sigma^+(x)], \quad C_2 = \frac{2}{a}, \quad (56)$$

$$\hat{\mathcal{O}}_3(x) = \frac{1}{a} [\sigma^-(x)U^\dagger(x)\sigma^+(x+1) - \sigma^-(x+1)U(x)\sigma^+(x)], \quad C_3 = \frac{2}{a}. \quad (57)$$

For $SU(2)$ they take the form

$$\hat{\mathcal{O}}_1(x) = \frac{1}{a} \sum_{\alpha} [\sigma_{\alpha}^+(x)\sigma_{\alpha}^-(x) - \sigma_{\alpha}^+(x+1)\sigma_{\alpha}^-(x+1)], \quad C_1 = \frac{4}{a}, \quad (58)$$

$$\hat{\mathcal{O}}_2(x) = \frac{1}{a} \sum_{\alpha, \beta} [\sigma_{\alpha}^-(x)\zeta_{\alpha\beta}(x)U_{\alpha\beta}^\dagger(x)\sigma_{\beta}^+(x+1) + \sigma_{\alpha}^-(x+1)\zeta_{\alpha\beta}(x)U_{\alpha\beta}(x)\sigma_{\beta}^+(x)], \quad C_2 = \frac{16}{a}, \quad (59)$$

$$\hat{\mathcal{O}}_3(x) = \frac{1}{a} \sum_{\alpha, \beta} [\sigma_{\alpha}^-(x)\zeta_{\alpha\beta}(x)U_{\alpha\beta}^\dagger(x)\sigma_{\beta}^+(x+1) - \sigma_{\alpha}^-(x+1)\zeta_{\alpha\beta}(x)U_{\alpha\beta}(x)\sigma_{\beta}^+(x)], \quad C_3 = \frac{16}{a}, \quad (60)$$

$$\hat{\mathcal{O}}_4(x) = \frac{2}{a} \sigma_1^-(x)\sigma_2^-(x), \quad C_4 = \frac{2}{a}, \quad (61)$$

where

$$\zeta_{11}(x) = \sigma_2^z(x), \quad \zeta_{12}(x) = \sigma_2^z(x)\sigma_1^z(x+1), \quad (62)$$

$$\zeta_{21}(x) = \mathbb{1}, \quad \zeta_{22}(x) = \sigma_1^z(x+1), \quad (63)$$

and the $U_{\alpha\beta}$ are decomposed as in equation (31).

For $SU(3)$ we have

$$\hat{\mathcal{O}}_1(x) = \frac{1}{a} \sum_{\alpha} [\sigma_{\alpha}^+(x)\sigma_{\alpha}^-(x) - \sigma_{\alpha}^+(x+1)\sigma_{\alpha}^-(x+1)], \quad C_1 = \frac{6}{a}, \quad (64)$$

$$\hat{\mathcal{O}}_2(x) = \frac{1}{a} \sum_{\alpha, \beta} [\sigma_{\alpha}^-(x)\zeta_{\alpha\beta}(x)U_{\alpha\beta}^\dagger(x)\sigma_{\beta}^+(x+1) + \sigma_{\alpha}^-(x+1)\zeta_{\alpha\beta}(x)U_{\alpha\beta}(x)\sigma_{\beta}^+(x)], \quad C_2 = \frac{130}{a}, \quad (65)$$

$$\hat{\mathcal{O}}_3(x) = \frac{1}{a} \sum_{\alpha, \beta} [\sigma_{\alpha}^-(x)\zeta_{\alpha\beta}(x)U_{\alpha\beta}^\dagger(x)\sigma_{\beta}^+(x+1) - \sigma_{\alpha}^-(x+1)\zeta_{\alpha\beta}(x)U_{\alpha\beta}(x)\sigma_{\beta}^+(x)], \quad C_3 = \frac{130}{a}, \quad (66)$$

$$\hat{\mathcal{O}}_4(x) = \frac{6}{a^{3/2}} \sigma_1^z(0)\sigma_2^z(0)\sigma_3^z(0)\sigma_1^z(1)\cdots\sigma_3^z(x-1)\sigma_1^-(x)\sigma_2^-(x)\sigma_3^-(x), \quad C_4 = \frac{6}{a^{3/2}}, \quad (67)$$

where again $\zeta_{\alpha\beta}(x)$ are strings of Z Pauli matrices analogous to the ones of the $SU(2)$ case, and the $U_{\alpha\beta}$ are decomposed as in equation (43). Notice that the baryon is a fermionic particle, which implies that the string of Pauli matrices $\sigma_1^z(0)\sigma_2^z(0)\sigma_3^z(0)\sigma_1^z(1)\cdots\sigma_3^z(x-1)$ does not cancel out as for bosonic particles.

We have thus provided explicit linear expansions of the interpolating operators in terms of unitary operators on qubit systems. The number of terms varies considerably from theory to theory and from particle to particle, but in all cases it is a constant. In the cases of $SU(2)$ and $SU(3)$, the quantities C_2 and C_3 are quite large because of the appearance of the operators $U_{\alpha\beta}$ in the expansion. This feature is specific of the Kogut-Susskind formulation. The number of gates required for each term in the expansion grows at most polynomially with the number of qubits dedicated to a lattice site.

V. QUANTUM CHROMODYNAMICS

We focus now on two-flavoured quantum chromodynamics in three dimensions. The first thing we need is to identify the continuum degrees of freedom with the lattice degrees of freedom. This is what we do in subsection V A. Then, in subsection V B we discuss the wave-packet creation of pions and nucleons.

A. Staggered fermions in three dimensions

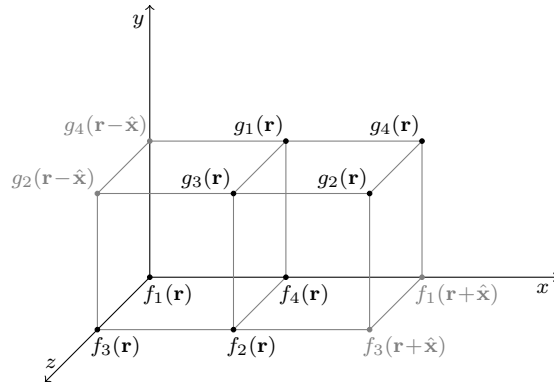


FIG. 2: Identification of the lattice fields with the continuum fields.

The staggered-fermion Hamiltonian in three dimensions reads

$$H_0 = \frac{1}{2a} \sum_{\mathbf{r}, \hat{\mathbf{n}}} [\xi^\dagger(\mathbf{r})\xi(\mathbf{r} + \hat{\mathbf{n}}) + \xi^\dagger(\mathbf{r} + \hat{\mathbf{n}})\xi(\mathbf{r})] \eta(\mathbf{r}, \hat{\mathbf{n}}) + m_0 \sum_{\mathbf{r}} (-1)^{x+y+z} \xi^\dagger(\mathbf{r})\xi(\mathbf{r}) \quad (68)$$

where $\mathbf{r} = (x, y, z)$ is a triplet of integers, $\hat{\mathbf{n}} \in \{\hat{\mathbf{x}}, \hat{\mathbf{y}}, \hat{\mathbf{z}}\}$ is a unit vector along a positive Cartesian axis, and

$$\eta(\mathbf{r}, \hat{\mathbf{x}}) = (-1)^z, \quad \eta(\mathbf{r}, \hat{\mathbf{y}}) = (-1)^x, \quad \eta(\mathbf{r}, \hat{\mathbf{z}}) = (-1)^y. \quad (69)$$

This Hamiltonian in the continuum limit describes two flavours of quarks, up and down for example, with the same mass $m_u = m_d = m_0$. Identifying the components of the two Dirac spinors $u(\mathbf{r})$ and $d(\mathbf{r})$ with the field $\xi(\mathbf{r})$ is not trivial, and several choices can be made up to $O(a)$ differences. We show here two possibilities based on [73, 74], where they perform a similar identification in momentum space.

First modify $\xi(\mathbf{r})$ by a phase,

$$\phi(\mathbf{r}) = i^{-x-z} A(y) D(x, z) \xi(\mathbf{r}), \quad (70)$$

with

$$A(y) = \frac{1}{\sqrt{2}} [i^{y-1/2} + (-i)^{y-1/2}], \quad D(x, z) = \frac{1}{2} [(-1)^x + (-1)^z + (-1)^{x+z+1} + 1]. \quad (71)$$

Then we identify ϕ at different sites with eight different fields as in figure 2,

$$\begin{aligned} f_1(\mathbf{r}) &= \phi(2\mathbf{r}), & f_2(\mathbf{r}) &= \phi(2\mathbf{r} + \hat{\mathbf{x}} + \hat{\mathbf{z}}), \\ f_3(\mathbf{r}) &= \phi(2\mathbf{r} + \hat{\mathbf{z}}), & f_4(\mathbf{r}) &= \phi(2\mathbf{r} + \hat{\mathbf{x}}) \\ g_1(\mathbf{r}) &= \phi(2\mathbf{r} + \hat{\mathbf{x}} + \hat{\mathbf{y}}), & g_2(\mathbf{r}) &= \phi(2\mathbf{r} + 2\hat{\mathbf{x}} + \hat{\mathbf{y}} + \hat{\mathbf{z}}), \\ g_3(\mathbf{r}) &= \phi(2\mathbf{r} + \hat{\mathbf{x}} + \hat{\mathbf{y}} + \hat{\mathbf{z}}), & g_4(\mathbf{r}) &= \phi(2\mathbf{r} + 2\hat{\mathbf{x}} + \hat{\mathbf{y}}). \end{aligned} \quad (72)$$

The two Dirac spinors are obtained with the transformations

$$\tilde{u} = \frac{1}{\sqrt{2}a^{3/2}}(f + g), \quad \tilde{d} = \frac{M}{\sqrt{2}a^{3/2}}(f - g), \quad (73)$$

$$u = \frac{1}{\sqrt{2}}(\tilde{u} - i\tilde{d}), \quad d = \frac{1}{\sqrt{2}}(-i\tilde{u} + \tilde{d}), \quad (74)$$

where

$$M = i \begin{pmatrix} \sigma_y & 0 \\ 0 & -\sigma_y \end{pmatrix} = \begin{pmatrix} 0 & 1 & 0 & 0 \\ -1 & 0 & 0 & 0 \\ 0 & 0 & 0 & -1 \\ 0 & 0 & 1 & 0 \end{pmatrix}. \quad (75)$$

We can put together the transformations as in

$$u = \frac{1}{2a^{3/2}}[(\mathbb{1} - iM)f + (\mathbb{1} + iM)g], \quad d = \frac{1}{2a^{3/2}}[(M - i\mathbb{1})f - (M + i\mathbb{1})g]. \quad (76)$$

In terms of the fields $u(\mathbf{r})$ and $d(\mathbf{r})$, the free fermion Hamiltonian reads

$$H_0 = \sum_{\mathbf{r}} a^3 \left[\frac{i}{2a} \sum_{\hat{\mathbf{n}}} \left[u^\dagger(\mathbf{r}) \alpha_n \Delta_{\hat{\mathbf{n}}} u(\mathbf{r}) + d^\dagger(\mathbf{r}) \alpha_n \Delta_{\hat{\mathbf{n}}} d(\mathbf{r}) \right] + \frac{i}{2a} \left[u^\dagger(\mathbf{r}) \beta \gamma_5 \Delta_{\hat{\mathbf{x}}\hat{\mathbf{y}}} u(\mathbf{r}) - d^\dagger(\mathbf{r}) \beta \gamma_5 \Delta_{\hat{\mathbf{x}}\hat{\mathbf{y}}} d(\mathbf{r}) \right] \right. \\ \left. + m_0 \left[u^\dagger(\mathbf{r}) \beta u(\mathbf{r}) + d^\dagger(\mathbf{r}) \beta d(\mathbf{r}) \right] \right] \quad (77)$$

where β , α_n and γ_5 are the usual Dirac matrices in the Dirac representation,

$$\beta = \begin{pmatrix} \mathbb{1} & 0 \\ 0 & -\mathbb{1} \end{pmatrix}, \quad \alpha_n = \begin{pmatrix} 0 & \sigma_n \\ \sigma_n & 0 \end{pmatrix}, \quad \gamma_5 = \begin{pmatrix} 0 & 1 \\ 1 & 0 \end{pmatrix}, \quad (78)$$

and

$$\Delta_{\hat{\mathbf{x}}} q(\mathbf{r}) = \begin{pmatrix} q_1(\mathbf{r} + \hat{\mathbf{x}}) - q_1(\mathbf{r}) \\ q_2(\mathbf{r}) - q_2(\mathbf{r} - \hat{\mathbf{x}}) \\ q_3(\mathbf{r} + \hat{\mathbf{x}}) - q_3(\mathbf{r}) \\ q_4(\mathbf{r}) - q_4(\mathbf{r} - \hat{\mathbf{x}}) \end{pmatrix}, \quad \Delta_{\hat{\mathbf{y}}} q(\mathbf{r}) = \frac{1}{2} \begin{pmatrix} q_1(\mathbf{r}) - q_1(\mathbf{r} - \hat{\mathbf{y}}) + q_1(\mathbf{r} + \hat{\mathbf{x}} + \hat{\mathbf{y}}) - q_1(\mathbf{r} + \hat{\mathbf{x}}) \\ q_2(\mathbf{r} + \hat{\mathbf{y}}) - q_2(\mathbf{r}) + q_2(\mathbf{r} - \hat{\mathbf{x}}) - q_2(\mathbf{r} - \hat{\mathbf{x}} - \hat{\mathbf{y}}) \\ q_3(\mathbf{r}) - q_3(\mathbf{r} - \hat{\mathbf{y}}) + q_3(\mathbf{r} + \hat{\mathbf{x}} + \hat{\mathbf{y}}) - q_3(\mathbf{r} + \hat{\mathbf{x}}) \\ q_4(\mathbf{r} - \hat{\mathbf{x}}) - q_4(\mathbf{r} - \hat{\mathbf{x}} - \hat{\mathbf{y}}) + q_4(\mathbf{r} + \hat{\mathbf{y}}) - q_4(\mathbf{r}) \end{pmatrix}, \\ \Delta_{\hat{\mathbf{z}}} q(\mathbf{r}) = \begin{pmatrix} q_1(\mathbf{r} + \hat{\mathbf{z}}) - q_1(\mathbf{r}) \\ q_2(\mathbf{r}) - q_2(\mathbf{r} - \hat{\mathbf{z}}) \\ q_3(\mathbf{r}) - q_3(\mathbf{r} - \hat{\mathbf{z}}) \\ q_4(\mathbf{r} + \hat{\mathbf{z}}) - q_4(\mathbf{r}) \end{pmatrix}, \quad \Delta_{\hat{\mathbf{x}}\hat{\mathbf{y}}} q(\mathbf{r}) = \frac{1}{2} \begin{pmatrix} q_1(\mathbf{r}) - q_1(\mathbf{r} - \hat{\mathbf{y}}) - q_1(\mathbf{r} + \hat{\mathbf{x}} + \hat{\mathbf{y}}) + q_1(\mathbf{r} + \hat{\mathbf{x}}) \\ q_2(\mathbf{r} + \hat{\mathbf{y}}) - q_2(\mathbf{r}) - q_2(\mathbf{r} - \hat{\mathbf{x}}) + q_2(\mathbf{r} - \hat{\mathbf{x}} - \hat{\mathbf{y}}) \\ q_3(\mathbf{r}) - q_3(\mathbf{r} - \hat{\mathbf{y}}) - q_3(\mathbf{r} + \hat{\mathbf{x}} + \hat{\mathbf{y}}) + q_3(\mathbf{r} + \hat{\mathbf{x}}) \\ q_4(\mathbf{r} - \hat{\mathbf{x}}) - q_4(\mathbf{r} - \hat{\mathbf{x}} - \hat{\mathbf{y}}) - q_4(\mathbf{r} + \hat{\mathbf{y}}) + q_4(\mathbf{r}) \end{pmatrix}. \quad (79)$$

Assuming we can expand the fields in Taylor series, in the continuum limit we have

$$\Delta_{\hat{\mathbf{x}}} q(\mathbf{r}) = a \partial_x q(\mathbf{r}) + O(a^2), \quad \Delta_{\hat{\mathbf{y}}} q(\mathbf{r}) = a \partial_y q(\mathbf{r}) + O(a^2), \quad \Delta_{\hat{\mathbf{z}}} q(\mathbf{r}) = a \partial_z q(\mathbf{r}) + O(a^2), \\ \Delta_{\hat{\mathbf{x}}\hat{\mathbf{y}}} q(\mathbf{r}) = O(a^2), \quad (80)$$

which confirms that the free staggered-fermion Hamiltonian describes two species of Dirac fermions in the continuum limit.

Another possible identification of the spinor components is the following. Based on figure 3, we set

$$f_1(\mathbf{r}) = \phi(2\mathbf{r}), \quad f_2(\mathbf{r}) = \phi(2\mathbf{r} + \hat{\mathbf{x}} + \hat{\mathbf{z}}), \quad f_3(\mathbf{r}) = \phi(2\mathbf{r} + \hat{\mathbf{z}}), \quad f_4(\mathbf{r}) = \phi(2\mathbf{r} + \hat{\mathbf{x}}) \\ g_1(\mathbf{r}) = \phi(2\mathbf{r} + \hat{\mathbf{x}} + \hat{\mathbf{y}}), \quad g_2(\mathbf{r}) = \phi(2\mathbf{r} + \hat{\mathbf{y}} + \hat{\mathbf{z}}), \quad g_3(\mathbf{r}) = \phi(2\mathbf{r} + \hat{\mathbf{x}} + \hat{\mathbf{y}} + \hat{\mathbf{z}}), \quad g_4(\mathbf{r}) = \phi(2\mathbf{r} + \hat{\mathbf{y}}), \quad (81)$$

and

$$u = \frac{1}{\sqrt{2}a^{3/2}}(f + g), \quad d = \frac{M}{\sqrt{2}a^{3/2}}(f - g). \quad (82)$$

Then the Hamiltonian takes the form

$$H_0 = \sum_{\mathbf{r}} a^3 \left[\frac{i}{2a} \sum_{\hat{\mathbf{n}}} \left[u^\dagger(\mathbf{r}) \alpha_n \Delta_{\hat{\mathbf{n}}} u(\mathbf{r}) + d^\dagger(\mathbf{r}) \alpha_n \Delta_{\hat{\mathbf{n}}} d(\mathbf{r}) \right] \right. \\ \left. + \frac{i}{2a} \left[u^\dagger(\mathbf{r}) \beta \gamma_5 \Delta_{\hat{\mathbf{x}}}^2 d(\mathbf{r}) + d^\dagger(\mathbf{r}) \beta \gamma_5 \Delta_{\hat{\mathbf{x}}}^2 u(\mathbf{r}) + iu^\dagger(\mathbf{r}) \beta \gamma_5 \Delta_{\hat{\mathbf{y}}}^2 d(\mathbf{r}) - id^\dagger(\mathbf{r}) \beta \gamma_5 \Delta_{\hat{\mathbf{y}}}^2 u(\mathbf{r}) \right] \right. \\ \left. + m_0 \left[u^\dagger(\mathbf{r}) \beta u(\mathbf{r}) + d^\dagger(\mathbf{r}) \beta d(\mathbf{r}) \right] \right], \quad (83)$$

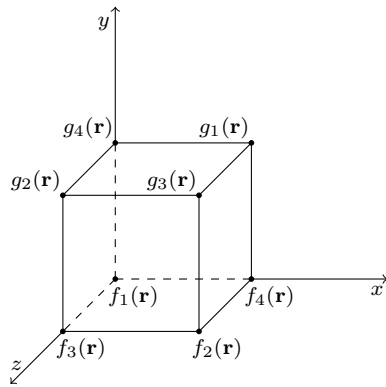


FIG. 3: Another identification of the lattice fields with the continuum fields.

where now

$$\begin{aligned}
 \Delta_{\hat{\mathbf{x}}} q(\mathbf{r}) &= \frac{1}{2} [q(\mathbf{r} + \hat{\mathbf{x}}) - q(\mathbf{r} - \hat{\mathbf{x}})], & \Delta_{\hat{\mathbf{x}}}^2 q(\mathbf{r}) &= \frac{1}{2} [q(\mathbf{r} + \hat{\mathbf{x}}) + q(\mathbf{r} - \hat{\mathbf{x}}) - 2q(\mathbf{r})], \\
 \Delta_{\hat{\mathbf{y}}} q(\mathbf{r}) &= \frac{1}{2} [q(\mathbf{r} + \hat{\mathbf{y}}) - q(\mathbf{r} - \hat{\mathbf{y}})], & \Delta_{\hat{\mathbf{y}}}^2 q(\mathbf{r}) &= \frac{1}{2} [q(\mathbf{r} + \hat{\mathbf{y}}) + q(\mathbf{r} - \hat{\mathbf{y}}) - 2q(\mathbf{r})], \\
 \Delta_{\hat{\mathbf{z}}} q(\mathbf{r}) &= \begin{pmatrix} q_1(\mathbf{r} + \hat{\mathbf{z}}) - q_1(\mathbf{r}) \\ q_2(\mathbf{r}) - q_2(\mathbf{r} - \hat{\mathbf{z}}) \\ q_3(\mathbf{r}) - q_3(\mathbf{r} - \hat{\mathbf{z}}) \\ q_4(\mathbf{r} + \hat{\mathbf{z}}) - q_4(\mathbf{r}) \end{pmatrix}.
 \end{aligned} \tag{84}$$

The main difference between the two identifications is that the first one is slightly more involved, but it avoids terms that mix the two flavours in the free theory. The second one is simpler, but the identified flavours are mixed. We give them both because it is not clear which one is more convenient. However, in the following, we consider only the first identification, equations (72) and (76), since it allows for a better identification of the flavours.

B. Interpolators in the Kogut-Susskind formulation

The Kogut-Susskind Hamiltonian for quantum chromodynamics on a three-dimensional cubic lattice is

$$H = H_M + H_K + H_E + H_B, \tag{85}$$

$$H_M = m_0 \sum_{\mathbf{r}} (-1)^{x+y+z} \xi^\dagger(\mathbf{r}) \xi(\mathbf{r}), \tag{86}$$

$$H_K = \frac{1}{2a} \sum_{\mathbf{r}, \hat{\mathbf{n}}} [\xi^\dagger(\mathbf{r}) U(\mathbf{r}, \hat{\mathbf{n}}) \xi(\mathbf{r} + \hat{\mathbf{n}}) + \xi^\dagger(\mathbf{r} + \hat{\mathbf{n}}) U^\dagger(\mathbf{r}, \hat{\mathbf{n}}) \xi(\mathbf{r})] \eta(\mathbf{r}, \hat{\mathbf{n}}), \tag{87}$$

$$H_E = \frac{g_0^2}{2a} \sum_{\mathbf{r}, \hat{\mathbf{n}}} E(\mathbf{r}, \hat{\mathbf{n}})^2, \tag{88}$$

$$H_B = -\frac{1}{2a^2 g_0^2} \sum_{\square} \text{tr} \left(P_{\square} + P_{\square}^\dagger \right), \tag{89}$$

where P_{\square} is a plaquette operator. The fields ξ , U and E are the $SU(3)$ fields discussed in the previous section. The encoding of the link Hilbert spaces does not differ from the one-dimensional case, while for the fermions it is more convenient to use a local encoding such as the generalized superfast encoding [75, 76]. This encoding was given only for operators made of products of an even number of fermionic operators. To create wave packets of a fermionic particle, such as the nucleons, we need to encode also odd fermionic operators. In the appendix we review the generalized superfast encoding and extend it to odd operators. In practice, the encoded versions of the operators ξ and ξ^\dagger are made of operators σ^\pm attached to a string of Pauli operators σ^x , σ^y and σ^z on other qubits. This is qualitatively similar to a Jordan-Wigner transformation, except that the strings of Pauli operators have different shapes depending on the details of the mapping.

Our goal here is to show how to write interpolating operators for the particles appearing in QCD, like the pion and the nucleons, in terms of qubit operators. Knowing the correspondence between the fields u and d and ξ , equations (72) and (76), we can use results from the literature on traditional lattice calculations [77–80]. However, the symmetries of the formulation used in [77–80] are different from the symmetries of the

Kogut-Susskind Hamiltonian. In particular, cubic and flavor symmetries are intertwined between each other for staggered fermions, which implies that spin and isospin mix together. On the other hand, spin and isospin are among the main symmetries used to classify and identify particles. As a consequence, identification of particles in the Kogut-Susskind formulation is possible only near the continuum limit, and up to $O(a)$ errors.

Pion interpolators are

$$\begin{aligned}\hat{\mathcal{O}}_{\pi^+}(\mathbf{r}) &= d^\dagger(\mathbf{r})\gamma_0\gamma_5u(\mathbf{r}), & \hat{\mathcal{O}}_{\pi^-}(\mathbf{r}) &= u^\dagger(\mathbf{r})\gamma_0\gamma_5d(\mathbf{r}), \\ \hat{\mathcal{O}}_{\pi^0}(\mathbf{r}) &= \frac{1}{\sqrt{2}}[u^\dagger(\mathbf{r})\gamma_0\gamma_5u(\mathbf{r}) - d^\dagger(\mathbf{r})\gamma_0\gamma_5d(\mathbf{r})].\end{aligned}\quad (90)$$

A proton interpolator is

$$\hat{\mathcal{O}}_p(\mathbf{r}) = \epsilon_{abc}[u_a^T(\mathbf{r})C\gamma_5d_b(\mathbf{r})]u_c(\mathbf{r}), \quad (91)$$

where $C = -i\alpha_y$ is the charge-conjugation matrix in the Dirac representation. The neutron interpolator is obtained by exchanging u and d .

These operators are not gauge invariant in the Kogut-Susskind formulation, as they involve products between ξ operators at different lattice sites as a consequence of the identifications in equation (72). We need to insert appropriate link operators to make them gauge invariant. The mesonic operators contain terms like $\xi^\dagger(2\mathbf{r})\xi(2\mathbf{r} + \hat{\mathbf{x}})$, which is made gauge invariant by $\xi^\dagger(2\mathbf{r})U(2\mathbf{r}, \hat{\mathbf{x}})\xi(2\mathbf{r} + \hat{\mathbf{x}})$. The baryonic operators contain terms like $\epsilon_{abc}\xi_a(2\mathbf{r})\xi_b(2\mathbf{r} + \hat{\mathbf{x}})\xi_c(2\mathbf{r} + 2\hat{\mathbf{x}} + \hat{\mathbf{y}})$, which is made gauge invariant by

$$\epsilon_{abc}U_{aa'}(2\mathbf{r} + \hat{\mathbf{x}}, -\hat{\mathbf{x}})\xi_{a'}(2\mathbf{r})\xi_b(2\mathbf{r} + \hat{\mathbf{x}})U_{cc'}(2\mathbf{r} + \hat{\mathbf{x}}, \hat{\mathbf{y}})U_{c'c''}(2\mathbf{r} + \hat{\mathbf{x}} + \hat{\mathbf{y}}, \hat{\mathbf{x}})\xi_{c'}(2\mathbf{r} + 2\hat{\mathbf{x}} + \hat{\mathbf{y}}). \quad (92)$$

The necessity of inserting link operators to restore gauge invariance, together with the transformations (72) and (76), makes writing interpolators in the Kogut-Susskind formulation extremely cumbersome. This becomes particularly relevant when we calculate the quantities C for these operators: We obtain approximately $C_{\pi^\pm} \sim 432/a^3$, $C_{\pi^0} = \sqrt{2}C_{\pi^\pm}$, and $C_p \sim 11500/a^{4.5}$. In a formulation such as one with Wilson fermions, in which each site contains the two spinors u and d , the corresponding quantities would be $C_{\pi^\pm} = 12/a^3$, $C_{\pi^0} = \sqrt{2}C_{\pi^\pm}$, and $C_p = 24/a^{4.5}$.

VI. CONCLUSIONS

Quantum computation opens the possibility to study real-time evolution of complex many-body quantum systems in a general and systematic way. However, much work is required on the experimental and theoretical sides to achieve meaningful simulations that are inaccessible with traditional techniques. In this manuscript, we aimed at solving the problem of preparing initial states suitable for scattering simulation, consisting of two wave packets moving on top of the vacuum. Simulating scattering of wave packets not only allows for the computation of physical quantities to be compared with experimental results, but also for disclosing what happens inside the collision.

Our method is a practical application of the Haag-Ruelle scattering theory developed in the context of axiomatic quantum field theory more than half a century ago. In reference [56] we showed how to create wave packets from the vacuum in scalar-field theories. Here we focused on lattice gauge theories, and increased gradually the level of difficulty, starting from a $U(1)$ theory in one dimension and ending with QCD in three dimensions with two flavors of quarks. We considered different kinds of particles, namely pions and nucleons in QCD.

Three ingredients are necessary to apply our method. First, we need to prepare the vacuum of the theory. This could be done with variational methods, like [52, 81], or with an adiabatic transformation [82]. Second, we need to know the spectrum of the theory. Near the continuum limit, this amounts to know the particle content and the particle masses. Finally, we need interpolating operators for the particles we aim at. These operators are built on a symmetry basis, and they should carry the quantum numbers of the particles. Our work is further extensible to other theories, formulations and particles, with the only requirement that there has to be a mass gap.

The creation of a wave packets with our strategy requires the use of LCU. This technique succeeds with a probability ρ that depends on the theory, on the wave packet, and on the particle. If we want to prepare n wave packets, the initial state preparations needs to be repeated on average $O(1/\rho^n)$ times to obtain the correct state for the simulation, so we can create only a small number of incoming wave packets. Fortunately, $n = 2$ is the most relevant case. The success probability seems to be the main limitation of our approach, but at least it does not affect the circuit depth, which is a favorable feature.

We chose to work in the Kogut-Susskind framework with staggered fermions. For QCD, we imported interpolators for the pions and the nucleons from the literature on traditional lattice calculations. We transformed these operators into operators in the staggered-fermion formulation, but this raises some problems. There are many possible choices for these transformations, with differences of the order of the lattice spacing, and none of them

respects the symmetries that determine the particles in the continuum. As a consequence, particle identification is more problematic, a well-known downside of staggered fermions. Furthermore, the success probability suffers significantly from the transformation of staggered fermions into Dirac spinors. The interpolating operators in the staggered-fermion formulation become long linear expansions of operators, with insertion of gauge fields to achieve gauge invariance. The resulting overheads in the success probability are $\sim 10^4$ for the pions, and $\sim 10^8$ for the nucleons. If we use Wilson fermions, the equivalent overheads are $\sim 10^2$.

In the future, the main issue that should be addressed is the success probability. Finding a different method to implement the creation operators with good probability would significantly improve our approach. Furthermore, it would be interesting to have detailed resource estimates, especially in the cases that have already been tested [50–52] to make a comparison between the different strategies. When the hardware is mature enough, it will be useful to test the method on a real quantum computer. It would also be important to have asymptotic estimates of the other approaches in the literature to determine which one is the most promising.

VII. ACKNOWLEDGMENTS

We are grateful for the support from FCT – Fundação para a Ciência e a Tecnologia (Portugal) – namely through Project No. UIDB/04540/2020 and Contract LA/P/0095/ 2020, as well as from projects QuantHEP and HQCC supported by the EU QuantERA ERA-NET Cofund in Quantum Technologies and by FCT (QuantERA/004/2021). Finally, M. T. thanks FCT for support through Grant No. PRT/BD/154668/2022. G. Q. acknowledges the support from FCT, through projects CEECIND/ 02474/2018, 2024.04456.CERN and FCT-Mobility/ 1312232346/2024-25.

Appendix: generalized superfast encoding of fermions

We review the generalized superfast encoding (GSE) of fermions into qubits [75]. In [76], this encoding was used to estimate the resource requirements for quantum simulation of lattice gauge theories such as quantum chromodynamics, showing a substantial improvement with respect to a Jordan-Wigner transformation. As presented in [75], the GSE allows for the representation of even fermionic operators only. As odd operators are necessary for the preparation of fermionic-particle wave packets, here we also show how they can be represented in the GSE. In this appendix we drop the Einstein convention for repeated indices.

1. Fermions

We first introduce some general facts about fermions. For a more detailed discussion see also [83]. Consider a system of N independent fermionic modes with annihilation operators a_1, \dots, a_N satisfying the usual anticommutation relations

$$\{a_I, a_J\} = 0, \quad \{a_I, a_J^\dagger\} = \delta_{IJ}. \quad (\text{A.1})$$

It is useful to introduce the Majorana modes as

$$\gamma_I^+ = a_I + a_I^\dagger, \quad \gamma_I^- = -i(a_I - a_I^\dagger). \quad (\text{A.2})$$

The Majorana modes are Hermitian, $\gamma_I^{\pm\dagger} = \gamma_I^\pm$, and satisfy the anticommutation relations

$$\{\gamma_I^\rho, \gamma_J^\sigma\} = 2\delta_{IJ}\delta_{\rho\sigma}, \quad (\text{A.3})$$

where $\rho, \sigma \in \{+, -\}$. In particular, note that $\gamma_I^{\pm 2} = 1$.

The Hilbert space of a fermionic system is spanned by all possible polynomials in the fermionic operators applied to the vacuum, and has dimension 2^N . The vacuum is defined as the state annihilated by all the annihilation operators,

$$a_I|0\rangle = 0, \quad \forall I. \quad (\text{A.4})$$

There are two subspaces of dimension 2^{N-1} each, usually called the even and the odd subspace. The even subspace is spanned by arbitrary combinations of products with an even number of fermionic operators applied to the vacuum. Similarly, the odd subspace is spanned by odd products of operators. Combinations of states in different subspaces are physically forbidden.

The even operators form a subalgebra generated by

$$B_I = -i\gamma_I^+ \gamma_I^-, \quad A_{IJ} = -i\gamma_I^+ \gamma_J^+. \quad (\text{A.5})$$

These operators satisfy the following relations:

$$B_I^\dagger = B_I, \quad A_{IJ}^\dagger = A_{IJ}, \quad B_I^2 = 1, \quad A_{IJ}^2 = 1, \quad A_{IJ} = -A_{JI}, \quad (\text{A.6})$$

$$B_I B_J = B_J B_I, \quad A_{IJ} B_K = (-1)^{\delta_{IK} + \delta_{JK}} B_K A_{IJ}, \quad A_{IJ} A_{KL} = (-1)^{\delta_{IK} + \delta_{IL} + \delta_{JK} + \delta_{JL}} A_{KL} A_{IJ}, \quad (\text{A.7})$$

$$A(\zeta) = i^s A_{\zeta(1)\zeta(2)} A_{\zeta(2)\zeta(3)} \dots A_{\zeta(s)\zeta(s+1)} = 1, \quad (\text{A.8})$$

where $\zeta : \{1, \dots, s+1\} \rightarrow \{1, \dots, N\}$ is a closed loop of length s with $\zeta(s+1) = \zeta(1)$. Furthermore we have

$$\prod_{I=1}^N B_I = 1 \quad \text{on the even subspace,} \quad (\text{A.9})$$

$$\prod_{I=1}^N B_I = -1 \quad \text{on the odd subspace.} \quad (\text{A.10})$$

Given an arbitrary γ_S^+ , we can write any other Majorana mode as a product of γ_S^+ and an even operator:

$$\gamma_S^- = i\gamma_S^+ B_S, \quad \gamma_I^+ = i\gamma_S^+ A_{SI}, \quad \gamma_I^- = -\gamma_S^+ A_{SI} B_I. \quad (\text{A.11})$$

This feature makes it very simple to implement an arbitrary fermionic operator on a qubit system once we have an encoding for the even operators.

2. Even operators in the GSE

To describe the GSE, we put the N fermionic modes on a connected graph with N vertices. We also require that each vertex be of even degree, and we assign an orientation to each edge. The graph can be chosen freely to suite a specific problem we want to address. For example, we might consider a Hamiltonian H and a graph $G = (V, E)$ such that H consists of terms acting nontrivially only on pairs of nearest neighbours on G , namely

$$H = \sum_{(I, J) \in E} H_{IJ}. \quad (\text{A.12})$$

We denote by $d(I)$ the degree of vertex $I \in V$, and we put $d(I)/2$ qubits on I . Next, we introduce $d(I)$ local Majorana modes for each vertex, $\gamma_{I1}, \dots, \gamma_{Id(I)}$, which satisfy the relations

$$\{\gamma_{Ii}, \gamma_{Ij}\} = 2\delta_{ij}, \quad (\text{A.13})$$

$$[\gamma_{Ii}, \gamma_{Jj}] = 0, \quad \text{if } I \neq J. \quad (\text{A.14})$$

We order the edges connected to vertex I as $1, \dots, d(I)$, and we attach the mode γ_{Ii} to the edge i . The local Majorana modes can be constructed with appropriate strings of Pauli matrices acting on the qubits of vertex I . From these modes we define the operators

$$\tilde{B}_I = (-i)^{d(I)/2} \gamma_{I1} \dots \gamma_{Id(I)} \quad \text{for each vertex } I, \quad (\text{A.15})$$

$$\tilde{A}_{IJ} = \epsilon_{IJ} \gamma_{Ii} \gamma_{Jj} \quad \text{for each edge } (I, J), \quad (\text{A.16})$$

where $\epsilon_{IJ} = 1$ if we follow the arrow when going from I to J , and $\epsilon_{IJ} = -1$ if we go in the opposite direction. The modes γ_{Ii} and γ_{Jj} in (A.16) are the two modes attached to the ends of edge (I, J) .

The operators defined in the expressions (A.15) and (A.16) satisfy the properties (A.6) and (A.7), but not the property (A.8), so we need to impose it. We define the qubit counterparts of the loop operators in (A.8) as

$$\tilde{A}(\zeta) = i^s \tilde{A}_{\zeta(1)\zeta(2)} \tilde{A}_{\zeta(2)\zeta(3)} \dots \tilde{A}_{\zeta(s)\zeta(s+1)} \quad (\text{A.17})$$

for any closed loop ζ of length s on the graph G , where now $\zeta(i)$ and $\zeta(i+1)$ are connected by an edge. The group \mathcal{S} generated by these loop operators form an Abelian group that commutes with \tilde{A}_{IJ} and \tilde{B}_I , and can be used as a stabilizer of the subspace

$$\mathcal{L} = \{|\psi\rangle : \tilde{A}(\zeta)|\psi\rangle = |\psi\rangle \text{ for all loops } \zeta\}. \quad (\text{A.18})$$

We can identify either the even or the odd subspace of the fermionic Hilbert space with the stabilized space \mathcal{L} , which has dimension 2^{N-1} . The operators \tilde{A}_{IJ} and \tilde{B}_I , when restricted to this subspace, satisfy also the property (A.8) by construction of \mathcal{L} , and give us a qubit representation of the algebra of even operators. Since G is a connected even-degree graph, there exists an Eulerian cycle, namely a loop η that utilizes every edge of the graph exactly once. For this loop we have

$$\prod_{I=1}^N \tilde{B}_I = \pm \tilde{A}(\eta), \quad (\text{A.19})$$

where the sign depends on our choice of the orientation of the edges. If our orientation produces a positive sign, \mathcal{L} represents the even subspace. Then, if we switch the direction of one arrow, we obtain a different subspace \mathcal{L} , which represents the odd subspace.

3. Odd operators in the GSE

In this section we show how to extend the generalized superfast encoding described in the previous section to also represent odd fermionic operators. Given a graph, a specific orientation of the edges gives one of many possible stabilized subspaces. Each of them can be identified either with the even or the odd subspace of the fermionic Hilbert space. Even operators, and their qubit representations, preserve these subspaces, while odd operators do not in the fermionic space and neither should their representation on the qubit space. Our goal is to find qubit operators representing the Majorana modes in (A.2) and (A.3). This representation should be compatible with the representation \tilde{A}_{IJ} and \tilde{B}_I of the previous section, at least on the stabilized subspace, and should make us jump from a space where equation (A.19) holds with the positive sign, to a space where it holds with the negative sign, and vice versa.

Consider again a graph as in the previous section, with every vertex of even degree, and take two vertices S and T connected by an edge. For every vertex I in the graph take a path ζ_{SI} from S to I that does not use the edge (S, T) , with $\zeta_{SI}(1) = S$ and $\zeta_{SI}(s) = I$. We can always find such paths following the Eulerian cycle η . Consider now the local Majorana mode on S attached to the edge (S, T) , which we can call γ_{S1} (up to relabeling of the modes). Motivated by

$$\gamma_I^+ = i\gamma_S^+ A_{SI}, \quad (\text{A.20})$$

$$\gamma_I^- = -\gamma_S^+ A_{SI} B_I, \quad (\text{A.21})$$

as a representation of the fermionic operators we take

$$\gamma_I^+ \rightarrow \hat{\gamma}_I^+ = \gamma_{S1} \tilde{A}(\zeta_{SI}), \quad (\text{A.22})$$

$$\gamma_I^- \rightarrow \hat{\gamma}_I^- = i\gamma_{S1} \tilde{A}(\zeta_{SI}) \tilde{B}_I, \quad (\text{A.23})$$

where

$$\tilde{A}(\zeta_{SS}) = 1, \quad (\text{A.24})$$

$$\tilde{A}(\zeta_{SI}) = i^{s-1} \tilde{A}_{\zeta_{SI}(1)\zeta_{SI}(2)} \tilde{A}_{\zeta_{SI}(2)\zeta_{SI}(3)} \dots \tilde{A}_{\zeta_{SI}(s-1)\zeta_{SI}(s)}. \quad (\text{A.25})$$

To see that this is a good representation of γ_I^\pm , first notice that

$$[\gamma_{S1}, \tilde{A}_{ST}] = 0, \quad (\text{A.26})$$

$$\{\gamma_{S1}, \tilde{A}_{SJ}\} = 0 \quad \text{if } J \neq T. \quad (\text{A.27})$$

The difference between the first and the second line is the reason for our choice of the paths ζ_{SI} . Then, from (A.6), (A.7) and (A.27), it is easy to see that $\hat{\gamma}_I^\pm$ satisfy the same anticommutation relations as γ_I^\pm .

The generators of the even algebra obtained from $\hat{\gamma}_I^+$ and $\hat{\gamma}_I^-$ are

$$\hat{B}_I = -i\hat{\gamma}_I^+ \hat{\gamma}_I^-, \quad \hat{A}_{IJ} = -i\hat{\gamma}_I^+ \hat{\gamma}_J^+, \quad (\text{A.28})$$

and it is straightforward to see that $\hat{B}_I = \tilde{B}_I$. Suppose now there is an edge (I, J) . In general, we have

$$\hat{A}_{IJ} \neq \tilde{A}_{IJ}. \quad (\text{A.29})$$

However, on the subspace $\mathcal{L} = \{|\psi\rangle : \tilde{A}(\zeta)|\psi\rangle = |\psi\rangle\}$, we have

$$\hat{A}_{IJ}|\psi\rangle = \hat{A}_{IJ}\tilde{A}(\zeta)|\psi\rangle. \quad (\text{A.30})$$

If we choose the loop ζ as the concatenation of ζ_{SI} , (I, J) and the reverse of ζ_{SJ} , we obtain $\hat{A}_{IJ}\tilde{A}(\zeta) = \tilde{A}_{IJ}$, and we can conclude

$$\hat{A}_{IJ}|\psi\rangle = \tilde{A}_{IJ}|\psi\rangle \quad \forall |\psi\rangle \in \mathcal{L}. \quad (\text{A.31})$$

From this we can see that the representation of the even algebra \tilde{B}_I and \tilde{A}_{IJ} is embedded in many representations of $\hat{\gamma}_I^+$ and $\hat{\gamma}_I^-$, one for each possible choice of the paths ζ_{SI} . When we restrict these representations to the stabilized space \mathcal{L} , they all coincide and give the representation of the even algebra introduced in [75].

To conclude, we need to see what happens when we act with an odd operator on a state in the stabilized subspace \mathcal{L} . Since all the operators \tilde{A}_{IJ} and \tilde{B}_I commute with the stabilizer operators $\tilde{A}(\zeta)$, the relations (A.26) and (A.27) imply

$$\{\hat{\gamma}_I^\pm, \tilde{A}(\zeta)\} = 0 \quad \text{if the loop } \zeta \text{ involves } (S, T); \quad (\text{A.32})$$

$$[\hat{\gamma}_I^\pm, \tilde{A}(\zeta)] = 0 \quad \text{if the loop } \zeta \text{ does not involve } (S, T). \quad (\text{A.33})$$

Suppose now that our initial choice of the arrows in the graph allows us to identify the space stabilized by $\{\tilde{A}(\zeta)\}$ with the even subspace,

$$\mathcal{L}^+ = \{|\psi\rangle : \tilde{A}(\zeta)|\psi\rangle = |\psi\rangle \text{ for all loops } \zeta\}, \quad \prod_{I=1}^N \tilde{B}_I = \tilde{A}(\eta) \quad (\text{A.34})$$

for an Eulerian cycle η . If we define

$$\bar{A}_{ST} = -\tilde{A}_{ST}, \quad (\text{A.35})$$

$$\bar{A}_{IJ} = \tilde{A}_{IJ} \quad \text{if } \{I, J\} \neq \{S, T\}, \quad (\text{A.36})$$

– which is equivalent to switching the arrow of (S, T) – then $\{\bar{A}(\zeta)\}$ is a stabilizer for the odd subspace,

$$\mathcal{L}^- = \{|\psi\rangle : \bar{A}(\zeta)|\psi\rangle = |\psi\rangle \text{ for all loops } \zeta\}, \quad \prod_{I=1}^N \tilde{B}_I = -\bar{A}(\eta). \quad (\text{A.37})$$

As a consequence of the relations (A.32) and (A.33), any odd operator makes us jump from \mathcal{L}^+ to \mathcal{L}^- , and vice versa. In virtue of this, we can conclude that the operators $\hat{\gamma}_I^\pm$, together with the two spaces \mathcal{L}^\pm provide us with a full representation of the fermionic Hilbert space and the associated algebra.

4. GSE for hypercubic lattices

In this work we use the GSE for $SU(N)$ gauge theories on hypercubic lattices with one flavour of fermions, which means that we have N independent fermionic modes on each site. In the one-dimensional case, the GSE essentially reduces to the Jordan-Wigner transformation. In d dimensions we use $N + d - 1$ qubits per lattice site. As an example, figure 4 depicts two neighbouring sites in an $SU(3)$ theory on a square lattice. The gray lines represent physical interaction terms in the Hamiltonian, and there is no such line between modes on the same site. The thick lines are edges of the graph we use for our encoding, and we also show the associated local Majorana modes on each mode. To obtain an interaction term between two modes, we simply choose the shortest path on the graph connecting the two modes, and the resulting encoded operator is in general a string of operators acting on the qubits involved in the path. Two out of three fermionic modes use one qubit each, the other modes use two qubits each. If mode I uses one qubit, we take as local Majorana modes

$$\gamma_{I1} = \sigma^x, \quad \gamma_{I2} = \sigma^y. \quad (\text{A.38})$$

If mode I uses two qubits, we take

$$\gamma_{I1} = \sigma^x \otimes \mathbb{1}, \quad \gamma_{I2} = \sigma^y \otimes \mathbb{1}, \quad \gamma_{I3} = \sigma^z \otimes \sigma^x, \quad \gamma_{I4} = \sigma^z \otimes \sigma^y. \quad (\text{A.39})$$

Adaptation of this example to an $SU(3)$ theory on a cubic lattice is straightforward.

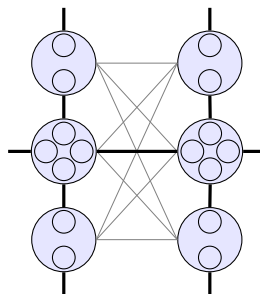


FIG. 4: GSE graph for $SU(3)$ on a square lattice. The gray lines represent physical interaction terms in the Hamiltonian, and there is no such line between modes on the same site. The thick lines are edges of the graph we use for our encoding, and we also show the associated local Majorana modes on each mode.

[1] B. Buyens, J. Haegeman, K. Van Acoleyen, H. Verschelde, and F. Verstraete, Matrix product states for gauge field theories, *Phys. Rev. Lett.* **113**, 091601 (2014), arXiv:1312.6654 [hep-lat].

[2] M. Rigobello, S. Notarnicola, G. Magnifico, and S. Montangero, Entanglement generation in $(1+1)D$ QED scattering processes, *Physical Review D* **104**, 10.1103/physrevd.104.114501 (2021), arXiv:2105.03445 [hep-lat].

[3] K. Marshall, R. Pooser, G. Siopsis, and C. Weedbrook, Quantum simulation of quantum field theory using continuous variables, *Physical Review A* **92**, 10.1103/physreva.92.063825 (2015), arXiv:1503.08121 [quant-ph].

[4] F. M. Surace and A. Leroose, Scattering of mesons in quantum simulators, *New Journal of Physics* **23**, 062001 (2021), arXiv:2011.10583 [cond-mat].

[5] P. I. Karpov, G. Y. Zhu, M. P. Heller, and M. Heyl, Spatiotemporal dynamics of particle collisions in quantum spin chains, *Phys. Rev. Res.* **4**, L032001 (2022), arXiv:2011.11624 [cond-mat].

[6] J. Vovrosh, R. Mukherjee, A. Bastianello, and J. Knolle, Dynamical hadron formation in long-range interacting quantum spin chains, *PRX Quantum* **3**, 10.1103/prxquantum.3.040309 (2022), arXiv:2204.05641 [cond-mat].

[7] R. Belyansky, S. Whitsitt, N. Mueller, A. Fahimniya, E. R. Bennewitz, Z. Davoudi, and A. V. Gorshkov, High-energy collision of quarks and mesons in the Schwinger model: From tensor networks to circuit QED, *Phys. Rev. Lett.* **132**, 091903 (2024), arXiv:2307.02522 [quant-ph].

[8] E. R. Bennewitz, B. Ware, A. Schuckert, A. Leroose, F. M. Surace, R. Belyansky, W. Morong, D. Luo, A. De, K. S. Collins, O. Katz, C. Monroe, Z. Davoudi, and A. V. Gorshkov, Simulating meson scattering on spin quantum simulators (2024), arXiv:2403.07061 [quant-ph].

[9] B. Fauseweh and J.-X. Zhu, Digital quantum simulation of non-equilibrium quantum many-body systems, *Quantum Information Processing* **20**, 10.1007/s11128-021-03079-z (2021), arXiv:2009.07375 [quant-ph].

[10] B. Fauseweh, Quantum many-body simulations on digital quantum computers: State-of-the-art and future challenges, *Nature Communications* **15**, 2123 (2024).

[11] A. J. Daley, I. Bloch, C. Kokail, S. Flannigan, N. Pearson, M. Troyer, and P. Zoller, Practical quantum advantage in quantum simulation, *Nature* **607**, 667 (2022).

[12] M. J. Savage, Quantum computing for nuclear physics (2023), arXiv:2312.07617 [nucl-th].

[13] L. H. Delgado-Granados, T. J. Krogmeier, L. M. Sager-Smith, I. Avdic, Z. Hu, M. Sajjan, M. Abbasi, S. E. Smart, P. Narang, S. Kais, A. W. Schlimgen, K. Head-Marsden, and D. A. Mazziotti, Quantum algorithms and applications for open quantum systems, *Chem. Rev.* **125**, 1823 (2025), arXiv:2406.05219 [quant-ph].

[14] R. Toshio, Y. Akahoshi, J. Fujisaki, H. Oshima, S. Sato, and K. Fujii, Practical quantum advantage on partially fault-tolerant quantum computer, *Phys. Rev. X* **15**, 021057 (2025), arXiv:2408.14848 [quant-ph].

[15] M. Lüscher, Volume dependence of the energy spectrum in massive quantum field theories, *Communications in Mathematical Physics* **105**, 153 (1986).

[16] C. W. Bauer, Z. Davoudi, A. B. Balantekin, T. Bhattacharya, M. Carena, W. A. de Jong, P. Draper, A. El-Khadra, N. Gemelke, M. Hanada, D. Kharzeev, H. Lamm, Y.-Y. Li, J. Liu, M. Lukin, Y. Meurice, C. Monroe, B. Nachman, G. Pagano, J. Preskill, E. Rinaldi, A. Roggero, D. I. Santiago, M. J. Savage, I. Siddiqi, G. Siopsis, D. Van Zanten, N. Wiebe, Y. Yamauchi, K. Yeter-Aydeniz, and S. Zorzetti, Quantum simulation for high-energy physics, *PRX Quantum* **4**, 027001 (2023), arXiv:2204.03381 [quant-ph].

[17] A. Avkhadiev, P. E. Shanahan, and R. D. Young, Accelerating lattice quantum field theory calculations via interpolator optimization using noisy intermediate-scale quantum computing, *Physical Review Letters* **124**, 080501 (2020), arXiv:1908.04194 [hep-lat].

[18] A. Avkhadiev, P. E. Shanahan, and R. D. Young, Strategies for quantum-optimized construction of interpolating operators in classical simulations of lattice quantum field theories, *Physical Review D* **107**, 054507 (2023), arXiv:2209.01209 [hep-lat].

[19] N. Klco, M. J. Savage, and J. R. Stryker, SU(2) non-abelian gauge field theory in one dimension on digital quantum computers, *Physical Review D* **101**, 074512 (2020), arXiv:1908.06935 [quant-ph].

[20] N. Mueller, A. Tarasov, and R. Venugopalan, Deeply inelastic scattering structure functions on a hybrid quantum computer, *Phys. Rev. D* **102**, 016007 (2020), arXiv:1908.07051 [hep-th].

[21] M. Kreshchuk, W. M. Kirby, G. Goldstein, H. Beauchemin, and P. J. Love, Quantum simulation of quantum field theory in the light-front formulation, *Physical Review A* **105**, 10.1103/physreva.105.032418 (2022), arXiv:2002.04016 [quant-ph].

[22] M. Echevarria, I. Egusquiza, E. Rico, and G. Schnell, Quantum simulation of light-front parton correlators, *Physical Review D* **104**, 10.1103/physrevd.104.014512 (2021), arXiv:2011.01275 [quant-ph].

[23] W. Qian, R. Basili, S. Pal, G. Luecke, and J. P. Vary, Solving hadron structures using the basis light-front quantization approach on quantum computers, *Physical Review Research* **4**, 10.1103/physrevresearch.4.043193 (2022), arXiv:2112.01927 [quant-ph].

[24] Z. Davoudi, N. Mueller, and C. Powers, Towards quantum computing phase diagrams of gauge theories with thermal pure quantum states, *Phys. Rev. Lett.* **131**, 081901 (2023), arXiv:2208.13112 [hep-lat].

[25] Y. Y. Atas, J. Zhang, R. Lewis, A. Jahanpour, J. F. Haase, and C. A. Muschik, SU(2) hadrons on a quantum computer via a variational approach, *Nature Communications* **12**, 10.1038/s41467-021-26825-4 (2021), arXiv:2102.08920 [quant-ph].

[26] Y. Y. Atas, J. F. Haase, J. Zhang, V. Wei, S. M. L. Pfaendler, R. Lewis, and C. A. Muschik, Simulating one-dimensional Quantum Chromodynamics on a quantum computer: Real-time evolutions of tetra- and pentaquarks, *Phys. Rev. Res.* **5**, 033184 (2023), arXiv:2207.03473 [quant-ph].

[27] C. F. Kane, D. M. Grabowska, B. Nachman, and C. W. Bauer, Overcoming exponential volume scaling in quantum simulations of lattice gauge theories (2022), arXiv:2212.04619 [hep-lat].

[28] H. Lamm, S. Lawrence, and Y. Yamauchi (NuQS), Parton physics on a quantum computer, *Physical Review Research* **2**, 10.1103/physrevresearch.2.013272 (2020), arXiv:1908.10439 [hep-lat].

[29] A. Mariani, S. Pradhan, and E. Ercolessi, Hamiltonians and gauge-invariant Hilbert space for lattice Yang-Mills-like theories with finite gauge group, *Physical Review D* **107**, 10.1103/physrevd.107.114513 (2023), arXiv:2301.12224 [quant-ph].

[30] E. Gustafson, Y. Zhu, P. Dreher, N. M. Linke, and Y. Meurice, Real-time quantum calculations of phase shifts using wave packet time delays, *Physical Review D* **104**, 10.1103/physrevd.104.054507 (2021), arXiv:2103.06848 [hep-lat].

[31] R. C. Farrell, I. A. Chernyshev, S. J. M. Powell, N. A. Zemlevskiy, M. Illa, and M. J. Savage, Preparations for quantum simulations of Quantum Chromodynamics in 1 + 1 dimensions. I. Axial gauge, *Physical Review D* **107**, 10.1103/physrevd.107.054512 (2023), arXiv:2207.01731 [quant-ph].

[32] R. C. Farrell, I. A. Chernyshev, S. J. M. Powell, N. A. Zemlevskiy, M. Illa, and M. J. Savage, Preparations for quantum simulations of Quantum Chromodynamics in 1 + 1 dimensions. II. Single-baryon β -decay in real time, *Physical Review D* **107**, 10.1103/physrevd.107.054513 (2023), arXiv:2209.10781 [quant-ph].

[33] J. Schuhmacher, G.-X. Su, J. J. Osborne, A. Gandon, J. C. Halimeh, and I. Tavernelli, Observation of hadron scattering in a lattice gauge theory on a quantum computer (2025), arXiv:2505.20387 [quant-ph].

[34] C. W. Bauer, B. Nachman, and M. Freytsis, Simulating collider physics on quantum computers using effective field theories, *Physical Review Letters* **127**, 10.1103/physrevlett.127.212001 (2021), arXiv:2102.05044 [hep-ph].

[35] D. Bluvstein, S. J. Evered, A. A. Geim, S. H. Li, H. Zhou, T. Manovitz, S. Ebadi, M. Cain, M. Kalinowski, D. Hangleiter, J. P. Bonilla Ataides, N. Maskara, I. Cong, X. Gao, P. Sales Rodriguez, T. Karolyshyn, G. Semeghini, M. J. Gullans, M. Greiner, V. Vuletić, and M. D. Lukin, Logical quantum processor based on reconfigurable atom arrays, *Nature* **626**, 58–65 (2023), arXiv:2312.03982 [quant-ph].

[36] Google Quantum AI and Collaborators, Quantum error correction below the surface code threshold, *Nature* **638**, 920–926 (2025), arXiv:2408.13687 [quant-ph].

[37] H. Lehmann, K. Symanzik, and W. Zimmermann, Zur formulierung quantisierter feldtheorien, *Il Nuovo Cimento (1955-1965)* **1**, 205 (1955).

[38] R. Haag, Quantum field theories with composite particles and asymptotic conditions, *Phys. Rev.* **112**, 669 (1958).

[39] D. Ruelle, On asymptotic condition in quantum field theory, *Helvetica Physica Acta* **35**, 147 (1962).

[40] A. Duncan, *The Conceptual Framework of Quantum Field Theory* (Oxford University Press, 2012).

[41] T. Li, W. K. Lai, E. Wang, and H. Xing (QuNu Collaboration), Scattering amplitude from quantum computing with reduction formula, *Phys. Rev. D* **109**, 036025 (2024), arXiv:2301.04179 [hep-ph].

[42] M. Kreshchuk, J. P. Vary, and P. J. Love, Simulating scattering of composite particles (2023), arXiv:2310.13742 [quant-ph].

[43] S. P. Jordan, K. S. M. Lee, and J. Preskill, Quantum algorithms for quantum field theories, *Science* **336**, 1130 (2012), arXiv:1111.3633 [quant-ph].

[44] S. P. Jordan, K. S. M. Lee, and J. Preskill, Quantum computation of scattering in scalar quantum field theories, *Quantum Info. Comput.* **14**, 1014–1080 (2014), arXiv:1112.4833 [hep-th].

[45] S. P. Jordan, K. S. M. Lee, and J. Preskill, Quantum algorithms for fermionic quantum field theories (2014), arXiv:1404.7115 [hep-th].

[46] G. K. Brennen, P. Rohde, B. C. Sanders, and S. Singh, Multiscale quantum simulation of quantum field theory using wavelets, *Physical Review A* **92**, 10.1103/physreva.92.032315 (2015), arXiv:1412.0750 [quant-ph].

[47] J. Barata, N. Mueller, A. Tarasov, and R. Venugopalan, Single-particle digitization strategy for quantum computation of a ϕ^4 scalar field theory, *Physical Review A* **103**, 10.1103/physreva.103.042410 (2021), arXiv:2012.00020 [hep-th].

[48] J. Liu, Z. Li, H. Zheng, X. Yuan, and J. Sun, Towards a variational Jordan–Lee–Preskill quantum algorithm, *Machine Learning: Science and Technology* **3**, 045030 (2022), arXiv:2109.05547 [quant-ph].

[49] N. A. Zemlevskiy, Scalable quantum simulations of scattering in scalar field theory on 120 qubits (2024), arXiv:2411.02486 [quant-ph].

[50] R. C. Farrell, M. Illa, A. N. Ciavarella, and M. J. Savage, Quantum simulations of hadron dynamics in the Schwinger model using 112 qubits, *Phys. Rev. D* **109**, 114510 (2024), arXiv:2401.08044 [quant-ph].

[51] R. C. Farrell, N. A. Zemlevskiy, M. Illa, and J. Preskill, Digital quantum simulations of scattering in quantum field theories using w states (2025), arXiv:2505.03111 [quant-ph].

[52] Z. Davoudi, C.-C. Hsieh, and S. V. Kadam, Scattering wave packets of hadrons in gauge theories: Preparation on a quantum computer, *Quantum* **8**, 1520 (2024), arXiv:2402.00840v3 [quant-ph].

[53] Z. Davoudi, C.-C. Hsieh, and S. V. Kadam, Quantum computation of hadron scattering in a lattice gauge theory (2025), arXiv:2505.20408 [quant-ph].

[54] Y. Chai, Y. Guo, and S. Kühn, Towards quantum simulation of meson scattering in a Z2 lattice gauge theory (2025), arXiv:2505.21240 [quant-ph].

[55] Y. Chai, A. Crippa, K. Jansen, S. Kühn, V. R. Pascuzzi, F. Tacchino, and I. Tavernelli, Entanglement production from scattering of fermionic wave packets: a quantum computing approach (2023), arXiv:2312.02272 [quant-ph].

[56] M. Turco, G. M. Quinta, J. Seixas, and Y. Omar, Quantum simulation of bound state scattering, *PRX Quantum* **5**, 020311 (2024), arXiv:2305.07692 [quant-ph].

[57] I. Raychowdhury and J. R. Stryker, Solving Gauss’s law on digital quantum computers with loop-string-hadron digitization, *Phys. Rev. Res.* **2**, 033039 (2020), arXiv:1812.07554v3 [hep-lat].

[58] I. Raychowdhury and J. R. Stryker, Loop, string, and hadron dynamics in $SU(2)$ Hamiltonian lattice gauge theories, *Phys. Rev. D* **101**, 114502 (2020), arXiv:1912.06133v2 [hep-lat].

[59] S. V. Kadam, I. Raychowdhury, and J. R. Stryker, Loop-string-hadron formulation of an $SU(3)$ gauge theory with dynamical quarks, *Phys. Rev. D* **107**, 094513 (2023), arXiv:2212.04490v2 [hep-lat].

[60] E. Mathew and I. Raychowdhury, Protecting gauge symmetries in the the dynamics of $SU(3)$ lattice gauge theories (2024), arXiv:2404.12158 [hep-lat].

[61] T. V. Zache, F. Hebenstreit, F. Jendrzejewski, M. K. Oberthaler, J. Berges, and P. Hauke, Quantum simulation of lattice gauge theories using Wilson fermions, *Quantum Science and Technology* **3**, 034010 (2018), arXiv:1802.06704 [cond-mat].

[62] G. Bergner, M. Hanada, E. Rinaldi, and A. Schäfer, Toward QCD on quantum computer: orbifold lattice approach, *Journal of High Energy Physics* **2024**, 234 (2024), arXiv:2408.13687 [quant-ph].

- [63] J. C. Halimeh, M. Hanada, S. Matsuura, F. Nori, E. Rinaldi, and A. Schäfer, A universal framework for the quantum simulation of yang-mills theory (2024), arXiv:2411.13161 [quant-ph].
- [64] S. Bachmann, W. Dybalski, and P. Naaijkens, Lieb–Robinson bounds, Arveson spectrum and Haag–Ruelle scattering theory for gapped quantum spin systems, *Annales Henri Poincaré* **17**, 1737 (2016), arXiv:1412.2970 [math-ph].
- [65] N. Klco and M. J. Savage, Digitization of scalar fields for quantum computing, *Physical Review A* **99**, 10.1103/phys-rev.a.99.052335 (2019), arXiv:1808.10378 [quant-ph].
- [66] Y. Tong, V. V. Albert, J. R. McClean, J. Preskill, and Y. Su, Provably accurate simulation of gauge theories and bosonic systems, *Quantum* **6**, 10.22331/q-2022-09-22-816 (2022), arXiv:2110.06942 [quant-ph].
- [67] A. M. Childs, R. Kothari, and R. D. Somma, Quantum algorithm for systems of linear equations with exponentially improved dependence on precision, *SIAM Journal on Computing* **46**, 1920 (2017), arXiv:1511.02306 [quant-ph].
- [68] G. Brassard, P. Høyer, M. Mosca, and A. Tapp, Quantum amplitude amplification and estimation, in *Quantum computation and information (Washington, DC, 2000)*, Contemp. Math., Vol. 305 (Amer. Math. Soc., Providence, RI, 2002) pp. 53–74, arXiv:quant-ph/0005055.
- [69] S. Capitani, Lattice perturbation theory, *Physics Reports* **382**, 113–302 (2003), arXiv:hep-lat/0211036v2.
- [70] A. Kan and Y. Nam, Lattice Quantum Chromodynamics and Electrodynamics on a universal quantum computer (2022), arXiv:2107.12769 [quant-ph].
- [71] T. Banks, L. Susskind, and J. Kogut, Strong-coupling calculations of lattice gauge theories: (1 + 1)-dimensional exercises, *Phys. Rev. D* **13**, 1043 (1976).
- [72] C. Hamer, Lattice model calculations for $SU(2)$ Yang-Mills theory in 1 + 1 dimensions, *Nuclear Physics B* **121**, 159 (1977).
- [73] L. Susskind, Lattice fermions, *Phys. Rev. D* **16**, 3031 (1977).
- [74] T. Banks, S. Raby, L. Susskind, J. Kogut, D. R. T. Jones, P. N. Scharbach, and D. K. Sinclair, Strong-coupling calculations of the hadron spectrum of quantum chromodynamics, *Phys. Rev. D* **15**, 1111 (1977).
- [75] K. Setia, S. Bravyi, A. Mezzacapo, and J. D. Whitfield, Superfast encodings for fermionic quantum simulation, *Phys. Rev. Res.* **1**, 033033 (2019), arXiv:1810.05274 [quant-ph].
- [76] M. Rhodes, M. Kreshchuk, and S. Pathak, Exponential improvements in the simulation of lattice gauge theories using near-optimal techniques (2024), arXiv:2405.10416 [quant-ph].
- [77] D. Leinweber, W. Melnitchouk, D. Richards, A. Williams, and J. Zanotti, Baryon spectroscopy in lattice QCD, in *Lattice Hadron Physics* (Springer Berlin Heidelberg, 2005) p. 71–112, arXiv:nucl-th/0406032.
- [78] S. Basak, R. Edwards, R. Fiebig, G. Fleming, U. Heller, C. Morningstar, D. Richards, I. Sato, and S. Wallace, Group-theoretical construction of extended baryon operators, *Nuclear Physics B - Proceedings Supplements* **140**, 287–289 (2005), arXiv:hep-lat/0409093.
- [79] T. Burch, C. Gattringer, L. Y. Glozman, C. Hagen, C. B. Lang, and A. Schäfer (BGR [Bern-Graz-Regensburg] Collaboration), Excited hadrons on the lattice: Mesons, *Phys. Rev. D* **73**, 094505 (2006), arXiv:hep-lat/0601026.
- [80] T. Burch, C. Gattringer, L. Y. Glozman, C. Hagen, D. Hierl, C. B. Lang, and A. Schäfer (BGR [Bern-Graz-Regensburg] Collaboration), Excited hadrons on the lattice: Baryons, *Phys. Rev. D* **74**, 014504 (2006), arXiv:hep-lat/0604019.
- [81] R. C. Farrell, M. Illa, A. N. Ciavarella, and M. J. Savage, Scalable circuits for preparing ground states on digital quantum computers: The Schwinger model vacuum on 100 qubits, *PRX Quantum* **5**, 020315 (2024), arXiv:2308.04481 [quant-ph].
- [82] M. D’Anna, M. K. Marinkovic, and J. C. P. Barros, Adiabatic state preparation for digital quantum simulations of QED in 1 + 1D (2024), arXiv:2411.01079 [hep-lat].
- [83] S. B. Bravyi and A. Y. Kitaev, Fermionic quantum computation, *Annals of Physics* **298**, 210 (2002), arXiv:quant-ph/0003137v1.